

Transcriptomes of Eight *Arabidopsis thaliana* Accessions Reveal Core Conserved, Genotype- and Organ-Specific Responses to Flooding Stress¹[OPEN]

Hans van Veen², Divya Vashisht^{2,3}, Melis Akman^{2,4}, Thomas Girke, Angelika Mustruph, Emilie Reinen, Sjon Hartman, Maarten Kooiker, Peter van Tienderen, M. Eric Schranz, Julia Bailey-Serres, Laurentius A.C.J. Voesenek, and Rashmi Sasidharan*

Plant Ecophysiology, Institute of Environmental Biology, Utrecht University, 3584 CH Utrecht, The Netherlands (H.v.V., D.V., E.R., S.H., M.K., J.B.-S., L.A.C.J.V., R.S.); Institute of Life Sciences, Scuola Superiore Sant'Anna, 56127 Pisa, Italy (H.v.V.); Institute for Biodiversity and Ecosystem Dynamics, University of Amsterdam, 1090 GE Amsterdam, The Netherlands (M.A., P.v.T.); Center for Plant Cell Biology, Botany, and Plant Sciences, University of California, Riverside, California 92521 (T.G., J.B.-S.); Department of Plant Physiology, Bayreuth University, 95447 Bayreuth, Germany (A.M.); and Biosystematics Group, Wageningen University, 6708 PB Wageningen, The Netherlands (M.E.S.)

ORCID IDs: 0000-0002-6709-6436 (S.H.); 0000-0001-6777-6565 (M.E.S.); 0000-0002-8568-7125 (J.B.-S.); 0000-0002-6940-0657 (R.S.).

Climate change has increased the frequency and severity of flooding events, with significant negative impact on agricultural productivity. These events often submerge plant aerial organs and roots, limiting growth and survival due to a severe reduction in light reactions and gas exchange necessary for photosynthesis and respiration, respectively. To distinguish molecular responses to the compound stress imposed by submergence, we investigated transcriptomic adjustments to darkness in air and under submerged conditions using eight *Arabidopsis* (*Arabidopsis thaliana*) accessions differing significantly in sensitivity to submergence. Evaluation of root and rosette transcriptomes revealed an early transcriptional and posttranscriptional response signature that was conserved primarily across genotypes, although flooding susceptibility-associated and genotype-specific responses also were uncovered. Posttranscriptional regulation encompassed darkness- and submergence-induced alternative splicing of transcripts from pathways involved in the alternative mobilization of energy reserves. The organ-specific transcriptome adjustments reflected the distinct physiological status of roots and shoots. Root-specific transcriptome changes included marked up-regulation of chloroplast-encoded photosynthesis and redox-related genes, whereas those of the rosette were related to the regulation of development and growth processes. We identified a novel set of tolerance genes, recognized mainly by quantitative differences. These included a transcriptome signature of more pronounced gluconeogenesis in tolerant accessions, a response that included stress-induced alternative splicing. This study provides organ-specific molecular resolution of genetic variation in submergence responses involving interactions between darkness and low-oxygen constraints of flooding stress and demonstrates that early transcriptome plasticity, including alternative splicing, is associated with the ability to cope with a compound environmental stress.

The environment that surrounds a plant changes constantly, often imposing constraints on metabolism that modify vegetative and reproductive development. Flooding can have a dramatic impact on plant performance; while it occurs regularly in some natural ecosystems, it is usually disastrous in controlled agricultural environments. Flooding restricts gas diffusion between submerged organs and the surrounding aquatic environment. The limited exchange of oxygen and CO₂ slows down aerobic respiration and photosynthesis (Mommer and Visser, 2005; Zabalza et al., 2009). Turbid and muddy floodwaters restrict light penetration, further compromising the photoautotrophic generation of critical carbohydrates (Vervuren et al., 2003). Finally, oxygen-deficient flooded soils often have a severely reduced redox potential and accumulate toxic compounds, which limit root growth (Armstrong and Armstrong, 2001).

Therefore, flooding is a compound stress, imposing multiple constraints on submerged plants. Despite this, marshes and river floodplains support a rich diversity of plant life that display a gradient of flood tolerance traits and responses (Van Eck et al., 2004; Voesenek et al., 2004). Studies on rice (*Oryza sativa*) and several wild species have identified two antithetical survival strategies, dependent on the selection pressure of their natural flooding regime. An escape response involving rapid shoot elongation allows plants to regain air contact by forming a snorkel during shallow and prolonged floods (Voesenek and Bailey-Serres, 2015). Deep or very short floods require a quiescent strategy, where a restriction of growth combined with conservation of energy expenditure and reserve utilization promotes survival until the floods recede (van Veen et al., 2014b). Fundamental knowledge of the genetic, physiological, and molecular regulation of these traits is not only of

general interest but essential to improve the tolerance of many economically relevant crops, most of which are very sensitive to floods (Voesenek et al., 2014). The genetic and molecular regulation of flood-adaptive strategies has been studied most extensively in semi-aquatic flood-tolerant species of the genera *Oryza*, *Rorippa*, and *Rumex* (Fukao et al., 2006; Hattori et al., 2009; Lee et al., 2009; Sasidharan et al., 2013; van Veen et al., 2013, 2014a; Narsai et al., 2015).

Our understanding of the flooding-induced low-oxygen and low-energy signaling networks also has benefited greatly from studies on flood-sensitive *Arabidopsis* (*Arabidopsis thaliana*). These investigations have identified the main players in energy and carbon signaling (Smeeckens et al., 2010; Ljung et al., 2015) and revealed whole-plant and cell type-specific transcriptional and translational adjustments induced by low-oxygen stress (Mustroph et al., 2009; Juntawong et al., 2014). Importantly, oxygen-dependent degradation of the group VII family of ethylene response factors via the N-end rule pathway of protein degradation has been identified as a molecular mechanism that translates oxygen availability into transcriptional reprogramming (Gibbs et al., 2011; Licausi et al., 2011; Weits et al., 2014). Recent studies also have revealed how this molecular hypoxic response is highly regulated and fine-tuned to maintain cellular homeostasis during low-oxygen conditions (Gibbs et al., 2014; Giuntoli et al., 2014; Gonzali et al., 2015).

Despite the progress in our understanding of flooding-induced signaling pathways, much remains to be discovered regarding the molecular mechanisms that cause variation in flooding tolerance across and within species (Voesenek and Bailey-Serres, 2015). Variation in flooding responses among natural plant populations is an important tool to identify the

underlying causal genes and processes (Xu et al., 2006; Magneschi et al., 2009; Chen et al., 2010; Campbell et al., 2015). Despite their relative intolerance to flooding stress, *Arabidopsis* accessions show considerable variation in their tolerance to complete submergence (Vashisht et al., 2011). Remarkably, this variation is not linked to differences in internal oxygen content or initial carbohydrate reserves, the two parameters generally considered to be essential for surviving flooding events.

The majority of studies investigating the molecular regulation of transcriptional reprogramming in response to changes in oxygen availability in *Arabidopsis* have relied on hypoxia and/or used agar-based seedling assays (Baena-González et al., 2007; Branco-Price et al., 2008; Bond et al., 2009; Christianson et al., 2009; Mustroph et al., 2009; Banti et al., 2010). However, in natural conditions, flooding results in a gradual decline in oxygen levels and often is accompanied by other physiological changes, such as a rapid buildup of the gaseous hormone ethylene (Voesenek and Sasidharan, 2013). Furthermore, flooding imposes distinct environmental constraints on the root and the shoot and, thereby, also elicits different physiological responses. Accordingly, an exploration of the shoot and root responses of flooded, soil-grown plants is more relevant to understanding flooding stress as experienced in the field.

Here, we characterized the early molecular response to darkness and flooding acclimation in eight different *Arabidopsis* genetic backgrounds (Supplemental Table S1), varying in their tolerance to complete submergence, using poly(A)⁺ mRNA sequencing (mRNAseq). The use of soil-grown plants subjected to submergence (in the dark) mimicked naturally flooded conditions in a highly controlled way, and the inclusion of a darkness-only (without submergence) treatment allowed us to simultaneously disentangle dark effects from submergence effects (Lee et al., 2011; Vashisht et al., 2011). Given the distinct carbohydrate and oxygen status of the root and shoot (rosette) tissues under these two stress conditions, these organs were analyzed separately, and then each organ response was compared with the other. This was performed for all eight accessions. Our data suggest an important role for gluconeogenesis in short-term stress acclimation, which includes alternative splicing (AS) of transcripts encoding key regulatory enzymes and quantitative transcriptional differences between tolerant and intolerant accessions. A conservative mode of energy and resource utilization via metabolic reprogramming and constrained growth contributes toward prolonged survival underwater. Shoot-specific flooding-induced transcriptional reprogramming was primarily growth related, whereas in the root, mainly plastidial and developmental processes changed. Our results provide insight into the interactive and additive effects of the different elements of flooding stress, present a detailed picture of early molecular events mediating stress acclimation, and identify putative novel aspects of flooding tolerance.

¹ This work was supported by the Netherlands Organization for Scientific Research (VENI grant no. 86312013 and ALW grant no. 82201007 to R.S.) and by the Centre for Biosystems Genomics (grant to L.A.C.J.V., R.S., and D.V.).

² These authors contributed equally to the article.

³ Present address: Gregor Mendel Institute of Molecular Plant Biology, Austrian Academy of Sciences, 1030 Vienna, Austria.

⁴ Present address: Department of Plant Microbial Biology, University of California, Berkeley, CA 94720.

* Address correspondence to r.sasidharan@uu.nl.

The author responsible for distribution of materials integral to the findings presented in this article in accordance with the policy described in the Instructions for Authors (www.plantphysiol.org) is: Rashmi Sasidharan (r.sasidharan@uu.nl).

H.v.V., D.V., M.A., J.B.-S., M.E.S., P.v.T., L.A.C.J.V., and R.S. conceived the research plans; J.B.-S., M.E.S., P.v.T., L.A.C.J.V., and R.S. supervised the experiments; D.V. and M.A. did most of the experiments; E.R. and S.H. provided technical assistance; H.v.V., D.V., M.A., T.G., and R.S. analyzed the data; R.S. and L.A.C.J.V. conceived the project; H.v.V. and R.S. wrote the article with contributions of all the authors; M.A., J.B.-S., M.E.S., P.v.T., and L.A.C.J.V. supervised and complemented the writing.

[OPEN] Articles can be viewed without a subscription.

www.plantphysiol.org/cgi/doi/10.1104/pp.16.00472

RESULTS

Early Transcriptomic Responses to Flooding and Darkness Are Largely Conserved among Accessions

To identify early transcriptome modifications upon flooding and dark-induced starvation, eight *Arabidopsis* genotypes (Cvi-0, Bay-0, Ita-0, Columbia-0 [Col-0; *gl1*], Kas-1, Lp2-6, Ws-2, and C24; Supplemental Table S1) were exposed to light (air + light [AL]), dark (air + darkness [AD]), or complete submergence (submerged + darkness [SD]) for 4 h (Fig. 1A). At this time point, the decline in oxygen levels caused by submergence had stabilized in both the root (less than 0.5 kPa) and petiole (approximately 6 kPa), as shown by oxygen microelectrode measurements in submerged *Arabidopsis* (Col-0) plants (Lee et al., 2011).

The mapping of mRNAseq reads to the Col-0 genome was successful, with 90.7% to 94.9% of the reads mapping to only a single genomic location. The number of mapped single-hit reads ranged from 20.5 to 43.9 million per library (Supplemental Table S2). Genes of very low abundance were removed from the analysis, leaving a final number of 21,940 genes. Multidimensional scaling (MDS) of the samples demonstrated a strong difference between root and shoot transcriptomes (Fig. 1B). A separate MDS analysis solely on shoot transcriptomes separated all three treatments over the x axis and the eight accessions over the y axis. A similar result was found for the root, but here, for each accession, the AD and SD samples clustered together, suggesting similarity between the dark and submergence transcriptional responses.

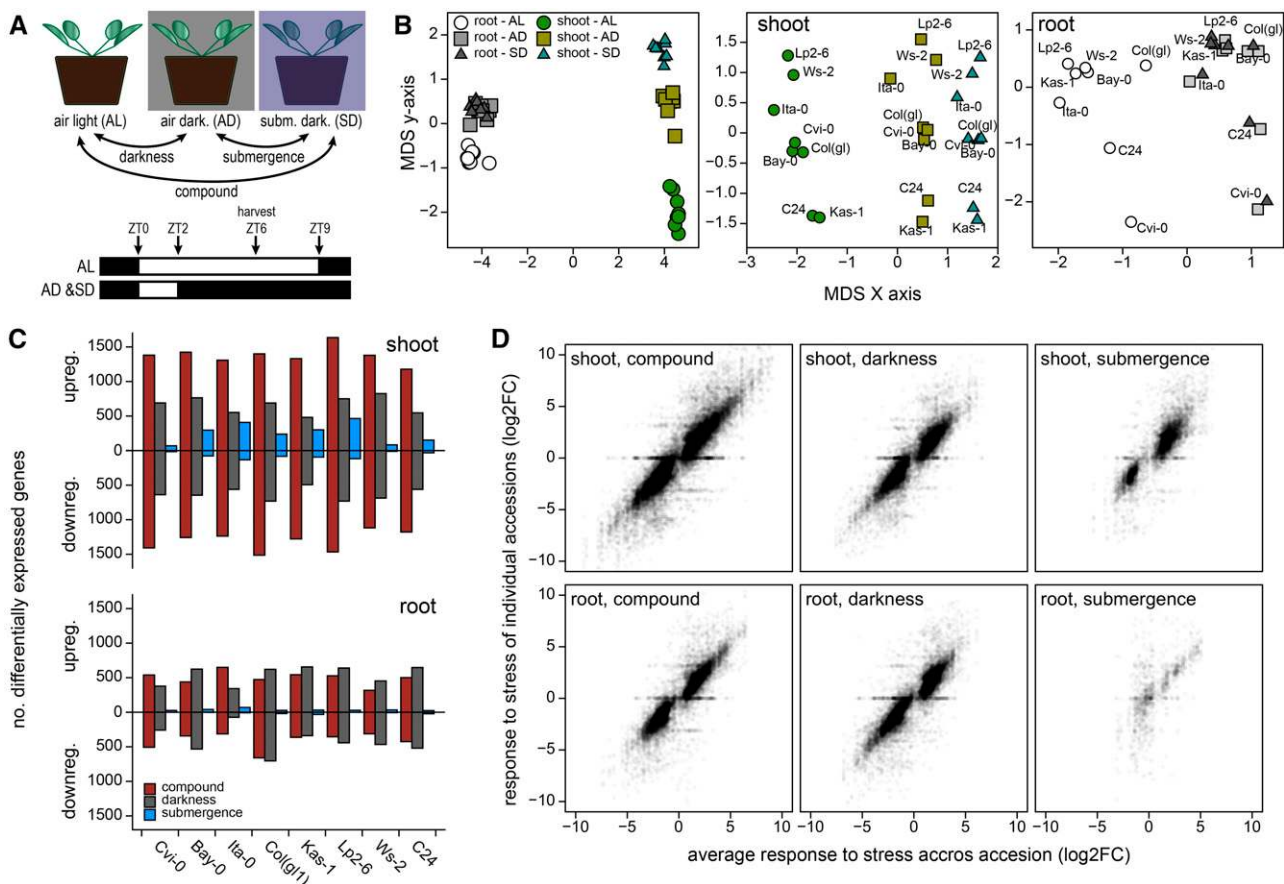


Figure 1. Transcriptional responses to compound, darkness, and submergence stress in eight *Arabidopsis* accessions. **A**, Schematic representation of the experimental setup, light cycle, and treatments used. *Arabidopsis* seedlings were grown until the 10-leaf stage (9-h photoperiod; Zeitgeber time [ZT], ZT0–ZT9). Plants then remained in control (AL) conditions or were transferred to SD or AD conditions 2 h after photoperiod initiation (ZT2). Shoot and root material from *Arabidopsis* seedlings exposed to AL, AD, and SD conditions for 4 h were harvested at ZT6 and used for mRNAseq. Black bars indicate darkness. Double-ended arrows indicate data sets compared to deduce the compound stress (AL versus SD), darkness (AL versus AD), and submergence (AD versus SD) differentially expressed genes (DEGs). **B**, MDS of all mRNAseq libraries, and of the shoot or root only, with distances based on the pairwise top-500 genes differing in fold change. **C**, Number of DEGs in shoots and roots ($P_{\text{adj.}} < 0.05$) in response to the compound, darkness, and submergence stress. **D**, Compound, darkness, and submergence responses of individual accessions compared with the weighted average response of all eight accessions. DEGs ($P_{\text{adj.}} < 0.05$) counted in **C** are depicted in the corresponding graph.

By comparing the transcriptomes of SD and AL, we identified genes that respond to the compound stress. Here, the compound stress is the effect of a combination of complete submergence and darkness, as often experienced by plants under naturally flooded conditions. The darkness response was teased apart from the compound stress using the AD-AL comparison. Finally, comparing SD with AD revealed a darkness-independent submergence response (Fig. 1A). Depending on the accession, 2,356 to 3,102 genes in the shoot were identified as being differentially expressed ($P_{\text{adj.}} < 0.05$) in response to the compound stress (Fig. 1C). Fewer DEGs were identified for the darkness response (975–1,481), and an even lower number were regulated significantly solely by submergence (84–581). Compared with the shoots, the compound response in the roots was of a lesser magnitude (782–1,133 DEGs), and a similar magnitude was found for darkness (415–1,325 DEGs). Furthermore, consistent with the MDS results (Fig. 1B) in the roots, there was hardly any effect of submergence only (26–76 DEGs). To investigate the overlap in the response among accessions for all identified DEGs, the accession-specific fold changes were plotted against the average fold change of all eight accessions (Supplemental Data Set S1, Sheets C and D). The strong correlations showed that the transcriptional adjustments of all accessions were very similar, especially for the compound and darkness effects (Fig. 1D; Supplemental Table S3). However, for the submergence effect, there was more variation among accessions, especially for the roots, where there was substantial scatter around a mean response of zero. For the shoot, two accessions, Cvi-0 and Ws-2, clearly showed a deviation from the average submergence response, as reflected in the much lower slopes (Cvi-0, 0.755; Ws-2, 0.759; average, 1.040; Supplemental Table S3). These also showed significantly overlapping responses to dark and compound stress in shoots (Supplemental Fig. S1) and the fewest shoot submergence DEGs of the accessions (Fig. 1C).

The natural variation in transcriptome responses was investigated further by identifying genes that responded in an accession-dependent manner ($P_{\text{accession} \times \text{treatment, adj.}} < 0.05$; Supplemental Data Set S1, Sheet E). In the root, 196, 288, and 137 genes were identified as varying significantly among accessions in their response to compound, darkness, and submergence, respectively, whereas in the shoot, 562, 311, and 181 genes were identified (Supplemental Fig. S2). To further investigate the conserved and accession-specific responses to compound, darkness, and submergence and highlight the implicit important processes and players, a Gene Ontology (GO) overrepresentation analysis was used.

Darkness Leads to Metabolic and Resource Adjustments; Submergence Is Characterized by the Regulation of Hormonal Processes

To identify the overall nature of the conserved transcriptomic responses, enrichment of GO terms was

investigated among genes that behaved similarly in all eight accessions ($P_{\text{accession} \times \text{treatment, adj.}} > 0.1$) and also showed a considerable response to the imposed stresses ($P_{\text{mean response, adj.}} < 0.01$, \log_2 fold change [FC] > 1.6 ; Fig. 2).

Typical overrepresented processes for conserved darkness and compound effects in all accessions were related to the down-regulation of energetically expensive cell wall construction, sulfur metabolism, starch biosynthesis (shoots only), and secondary metabolism. Interestingly, Suc and Fru responses and trehalose phosphate synthase activity terms were overrepresented among up-regulated genes in both the root and shoot. Not surprisingly, the response to absence of light category also was overrepresented among the up-regulated genes in both shoot and root in dark and compound stress. We also identified cellular response to iron ion overrepresentation among down-regulated genes in the root in response to the compound stress. The GO analyses further revealed changes associated with nitrogen metabolism. This included the nitrate transport, amino acid transport, and Leu catabolic process terms that were overrepresented among up-regulated genes in the shoot. Together, these results suggested a fundamental change in the metabolic network in response to the applied stresses.

Compared with the darkness and compound effects, a lower number of significantly enriched GO terms were identified for submergence stress only. The up-regulated genes, as expected, included anaerobic metabolism, hypoxic response, and Suc synthase activity. Other uniquely submergence-responsive GO categories were hormone related (ethylene, auxin, and abscisic acid [ABA]), indicating transcriptional regulation associated with these hormonal cascades that is not activated by the more metabolically determined darkness effects.

To characterize the accession-dependent responses, GO overrepresentation analysis also was performed on genes that varied in their treatment responses ($P_{\text{accession} \times \text{treatment, adj.}} < 0.05$; Supplemental Fig. S3). The GO terms enriched among these genes encompassed a wide range of categories. These were mostly associated with photosynthesis and metabolism (lipids, amino acids, and sulfur) and biotic defense. There was some overlap in the GO enrichment categories between the conserved and accession-dependent responses. This indicated a strong regulation of the related processes, but in varying levels of conservation among accessions.

The Compound Stress Response Is an Amplified Darkness Response in the Shoot

In nature, severe flooding often consists of submergence coupled with very low light intensities. Here, we investigated the relative contribution of darkness and submergence toward the final compound flooding stress response. In the shoot, the direct comparison of the compound and darkness responses showed a strong positive correlation (Fig. 3A). The steep slope

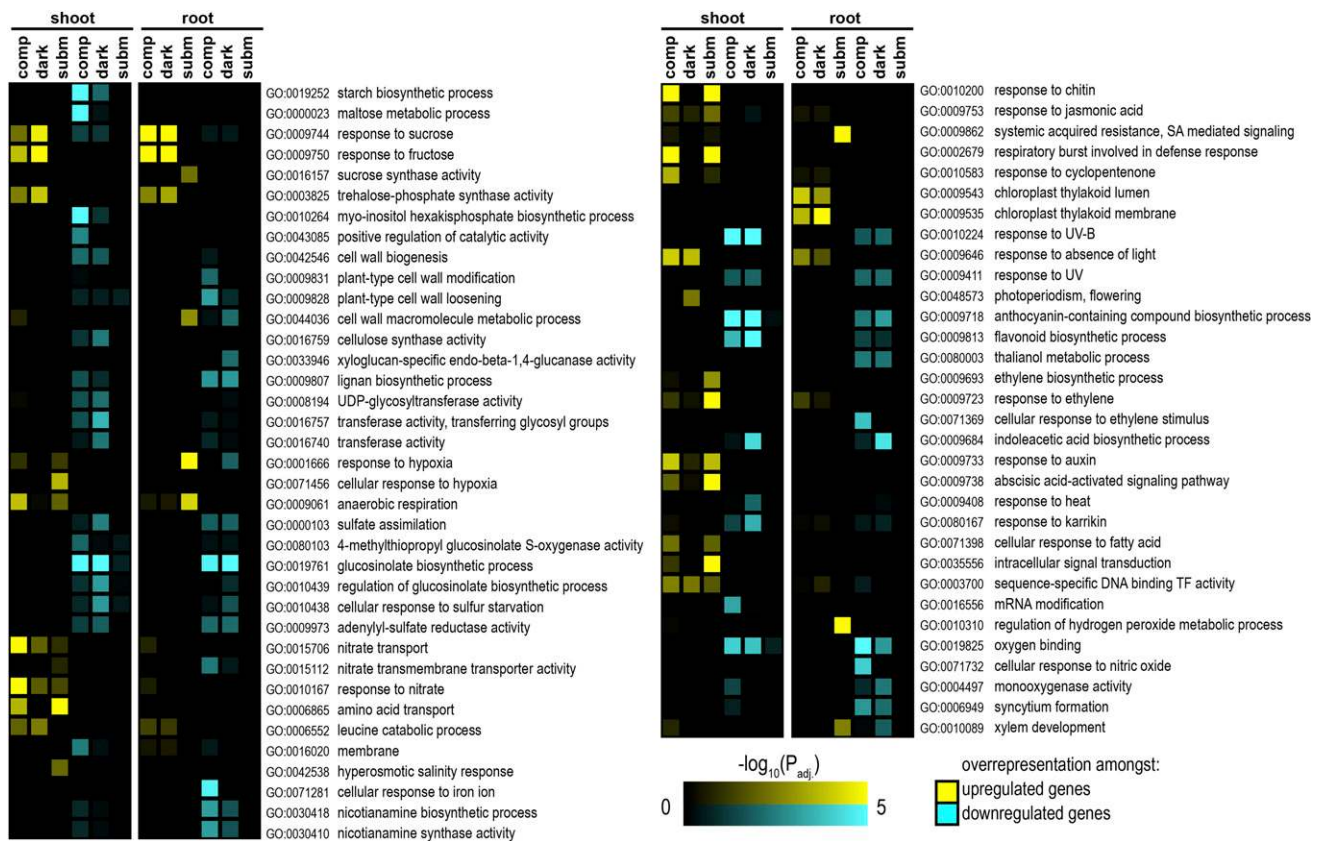


Figure 2. GO terms overrepresented in the conserved compound, darkness, and submergence responses of the eight accessions. Overrepresentation was determined for genes where the average response across accessions was mean \log_2 FC > 1.6 and $P_{adj.} < 0.01$ and where variation in the response between accessions was absent ($P_{accession \times treatment, adj.} > 0.1$). GO terms with $P_{adj.} < 0.01$ are shown.

suggested that the compound response was similar to the dark response but was enhanced by the addition of submergence. A similar comparison of the compound versus darkness response of the root also showed a strong correlation. However, no additional effect of submergence on the global transcriptomic response was observed (i.e. the compound and darkness effects were of similar magnitude; Fig. 3A).

To further characterize the gene categories constituting the relationships identified above, we grouped genes that were coexpressed and, therefore, are potentially members of same or similarly regulated gene pathways. We used WGCNA (Langfelder and Horvath, 2008) to perform a comparative analysis of gene networks among the three conditions (AL, AD, and SD). Fifteen and eight coexpression modules were identified for the shoot and root, respectively, where each module consists of genes that show largely similar expression patterns across the different accessions and conditions (Fig. 3B; Supplemental Fig. S4). GO term enrichment was investigated subsequently for the identified modules (Supplemental Data Set S1, Sheets F and G).

For both the root and shoot, two very large gene coexpression modules were identified, namely R01,

R02, S01, and S02 (Fig. 3B). The R01 and R02 modules both showed consistent changes in expression upon darkness (either an increase or decrease) in all accessions but no change upon submergence. However, R01 and R02 differed in the constitutive expression levels of the accessions (Fig. 3C). These were enriched in GO terms related to metabolism, such as glycolysis/gluconeogenesis, fatty acid breakdown, acetyl-CoA, and secondary metabolism (glucosinolates and isopentenyl pyrophosphate/methylerythritol pathway), but also included sugar transport and signaling. Enrichment terms also indicated a role for jasmonic acid and brassinosteroids in the root upon darkness and compound stress (Fig. 3C).

By comparison, the genes in module S01 were expressed similarly in all accessions and only had a darkness response and no additional submergence effect (Fig. 3D). This module was enriched for GO categories related to photoperiod, lipid breakdown (in the peroxisome), protein transport (required for peroxisome function), and sugar-mediated signaling (Fig. 3D; Supplemental Data Set S1, Sheet G). Gene expression patterns in the other large shoot module, S02, demonstrated the amplified dark response by submergence for

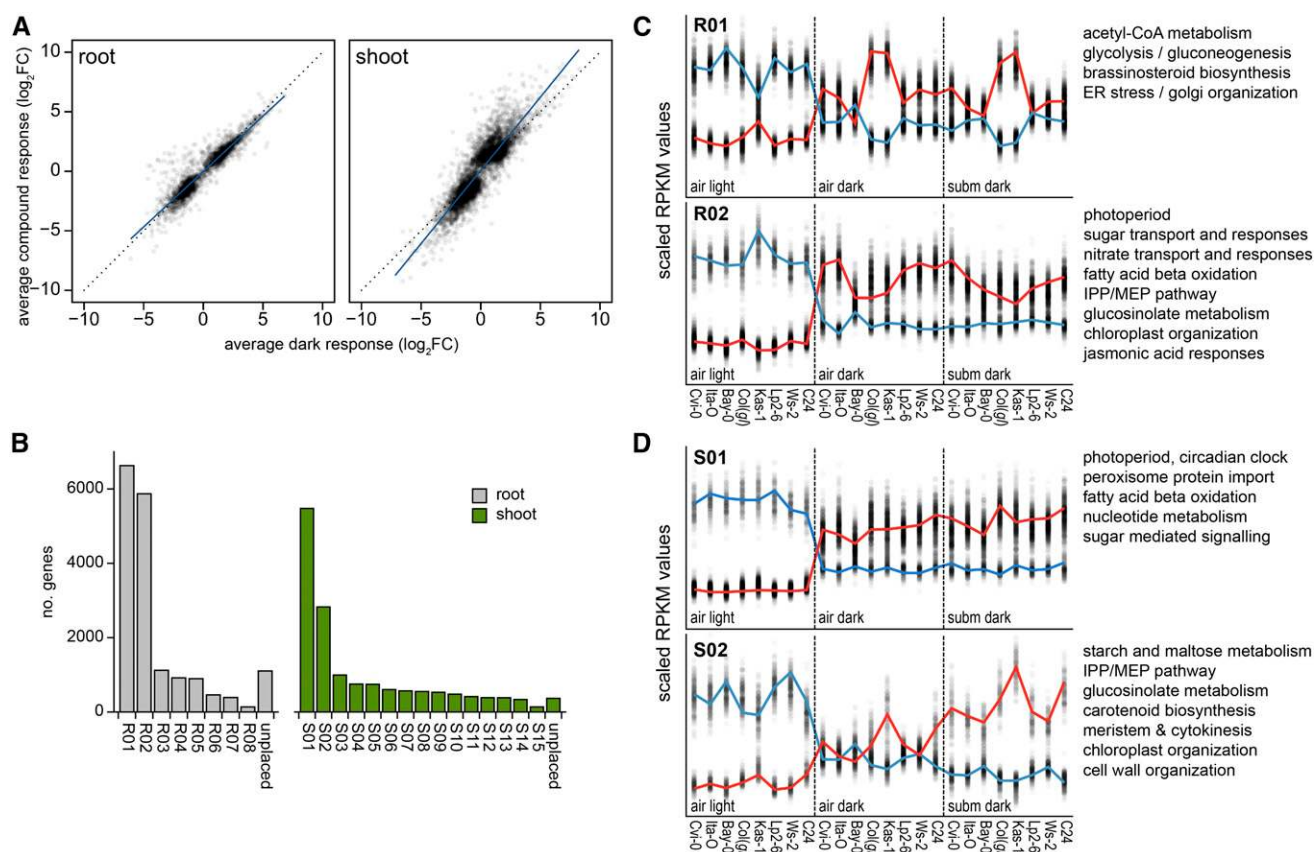


Figure 3. Cumulative effects of darkness and submergence and Weighted Gene Coexpression Network Analysis (WGCNA) clustering. **A**, Comparison of the compound and dark responses of roots and shoots. Mean responses to treatments are plotted for both the x and y variables. Responses for individual accessions can be found in Supplemental Figure S1. The black dotted line represents $y = x$, and the blue solid line is the regression of the data for the root ($y = -0.02 + 0.93 \times x$; $r^2 = 0.88$) and shoot ($y = -0.06 + 1.23 \times x$; $r^2 = 0.84$). **B**, Gene coexpression modules and their sizes as identified by WGCNA. Gene modules show similar expression patterns across the three treatments and eight accessions. Roots (R) and shoots (S) were analyzed separately. Not all genes included in the analysis could be placed in a module of coexpressed genes, and these were unplaced. **C** and **D**, Mean and variation-centered reads per kilobase per million (RPKM) values of the largest two root (**C**) and shoot (**D**) coexpression modules identified by WGCNA. The top 12% of genes with the highest module membership score are shown. The blue and red lines reflect the trends of the gene with the strongest positive and negative correlation to the mean module behavior, respectively. The remaining modules are visualized in Supplemental Figure S4. To the right of each module are representative terms related to the identified enriched GO terms. The complete GO analysis is given in Supplemental Data Set S1, Sheets F and G. ER, Endoplasmic reticulum; IPP/MEP, isopentenyl pyrophosphate/methylerythritol.

the compound stress. Enriched GO terms included starch and secondary metabolism. Furthermore, enrichment was found for the processes of cell division and meristem function. No clear submergence-specific module was identified in the shoot or the root (Supplemental Fig. S4), likely because of the relatively small number of genes affected by submergence only (Fig. 1C).

Root- and Shoot-Specific Treatment-Responsive Genes Are Associated with Photosynthesis and Growth Regulation

Since the organ-specific responses to the treatments were more distinct than the response across accessions (Fig. 1B), these differences were explored further. First, DEGs that were dependent on the organ (i.e. genes with

a significant organ-treatment interaction) were identified ($P_{\text{organ} \times \text{treatment, adj.}} < 0.05$; Supplemental Fig. S5A; Supplemental Data Set S, Sheet H). These organ-dependent treatment responses were largely conserved across accessions (Supplemental Fig. S5B). Genes with an organ-treatment interaction ($P_{\text{organ} \times \text{treatment, adj.}} < 0.05$) and a significant treatment effect ($P_{\text{adj.}} < 0.05$) in only one organ for six or more accessions were identified and designated as either root- or shoot-specific response genes (Fig. 4A, red and blue dots, respectively). The number of shoot-specific genes identified for the compound, darkness, and submergence effect were 340, 33, and 13, respectively. Fewer root-specific genes were found: 59 and 48 for compound and darkness, respectively. There were no root-specific genes for the submergence response. Clustering of the

organ-specific genes identified a strong overlap between the three treatments (Fig. 4B). The compound response of the root-specific genes mirrored the darkness response, whereas shoot-specific genes of the compound response also illustrated the amplification of the darkness response by submergence.

There was a very strong overlap in shoot-specific genes between the compound, darkness, and submergence responses (Fig. 4B). Among these shoot-specific genes were those involved in hormonal metabolism and signaling, cell growth, and cell wall modification (Supplemental Data Set S1, Sheet H). For example, the mRNA levels of *NINE-CIS-EPOXYCAROTENOID DIOXYGENASE4*, catalyzing a crucial enzymatic step in ABA biosynthesis, was down-regulated, whereas ethylene (*1-AMINOCYCLOPROPANE-1-CARBOXYLATE SYNTHASE* and *1-AMINOCYCLOPROPANE-1-CARBOXYLATE OXIDASE*), GA (*GA 20-OXIDASE* and *GA 2-OXIDASE6*), and cytokinin (*CYTOKININ OXIDASE3*) metabolism enzymes were up-regulated. Downstream signaling components typical for auxin and brassinosteroids were among the up-regulated shoot-specific genes (*SMALL AUXIN UP-REGULATED [SAUR]* and *SAUR-LIKE* genes, *AUXIN-REGULATED GENE INVOLVED IN ORGAN SIZE*, *BXR1 SUPPRESSOR1*, *BR-ENHANCED EXPRESSION1*, and the *BZR1*-interacting *GENERAL REGULATORY FACTOR8*). Downstream effector genes such as cell wall-modifying enzymes with shoot-specific regulation (in both directions) included six genes involved in pectin esterification, two cell wall-loosening expansins, and eight xyloglucan endotransglucosylase/hydrolases.

Several plant developmental control and light signaling genes also were among the regulated shoot-specific genes (Supplemental Data Set S1, Sheet H). These included the genes *SQUAMOSA PROMOTER-LIKE11* responsible for seedling to juvenile to adult stage transitions (Huijser and Schmid, 2011) but also *CLAVATA3/ESR-RELATED16 (CLE16)*, *CLE6*, and *CLAVATA2*, which are regulatory factors in shoot apical meristem activity (Gaillochet et al., 2015). Among the light signaling genes were the negative regulators of photomorphogenesis *B-BOX DOMAIN PROTEIN18*, *SPA1-RELATED3*, and *FAR-RED ELONGATED HYPOCOTYL1* required for phyA signaling (Li et al., 2011). The photoperiod-related gene *FLOWERING bHLH3* and the circadian clock gene *PSEUDO-RESPONSE REGULATOR9* also were among the compound shoot-specific DEGs.

In the root, the compound and dark responses were identical, and no submergence root-specific genes were identified (Fig. 4, A and B). Interestingly, the root-specific up-regulated genes consisted mainly of chloroplast-localized and photosynthesis-related genes (Supplemental Data Set S1, Sheet H). This included at least seven genes involved in photosystem biosynthesis and maintenance, five additional proteins localized to the chloroplast, one essential for chlorophyll biosynthesis, and two involved in photorespiration. Only a few root-specific down-regulated mRNAs were identified, which included two nitrate transporters and

a MATE efflux protein. In summary, mostly growth, developmental, and hormonal regulatory gene transcripts were stress induced in the shoot, while chloroplast-encoded and photosynthesis-associated genes dominated the root-specific DEGs.

Induction of the Core Hypoxia Gene Set Is Organ Independent Only When the Darkness Component Is Excluded

Previous studies identified 51 genes that were up-regulated in Arabidopsis seedlings upon hypoxic stress, regardless of organ or cell type (Mustroph et al., 2009), and that are frequently used as core hypoxia response markers. In soil-grown plants, roots and shoots have distinct oxygen profiles under both control and submerged conditions. Soil-grown roots of Arabidopsis are constitutively hypoxic, and upon submergence, internal oxygen levels drop further from 6% to approximately 0% pO₂ KPa within 3 h (Lee et al., 2011). Although the oxygen dynamics of Arabidopsis leaf blades is unknown, the petiole goes from 17% to 6% pO₂ KPa upon submergence in the same time span. We investigated the expression pattern of the 51 cell type-independent hypoxia-responsive genes in the context of the severe and mild low oxygen levels in the submerged root and shoot, respectively (Fig. 4, A, green dots, and C).

A majority of core hypoxia genes were regulated in both shoots and roots upon compound, darkness, or submergence. However an organ-independent hypoxia signature response, involving the up-regulation of most of the 51 genes, was observed only for the submergence response (when the effects of darkness were excluded; Fig. 4C). This submergence response also was very similar in magnitude in the roots and shoots. In contrast, for the compound response, 18 of the 51 core hypoxia genes were classified as shoot specifically regulated ($P_{\text{organ} \times \text{treatment, adj.}} < 0.05$ in six or more accessions). Only a few of the hypoxia marker genes were classified as root or shoot specific upon darkness. However, during darkness, the root had a predominant down-regulation of most core hypoxia genes, and in the shoot, several were dark up-regulated in Cvi-0 and Ws-2 (Fig. 4C). Interestingly, a small subset was induced upon darkness in both organs (AT4G27450, AT1G33055, AT1G19530, AT4G39675, AT5G61440, and AT3G61060). These were identified previously as induced by carbon starvation (Usadel et al., 2008) and include *EXORDIUM LIKE1* (Schröder et al., 2011). In conclusion, it is clear that, for the compound response, the behavior toward darkness is an important determinant of the difference between the shoot and root for these cell type-independent hypoxia marker genes (Fig. 4, A and C).

Conserved AS Events Indicate an Additional Layer of Regulation in the Adaptation to Compound, Darkness, and Submergence Stresses

Using mRNAseq as a platform, we were able to investigate transcriptome reconfiguration at the mRNA

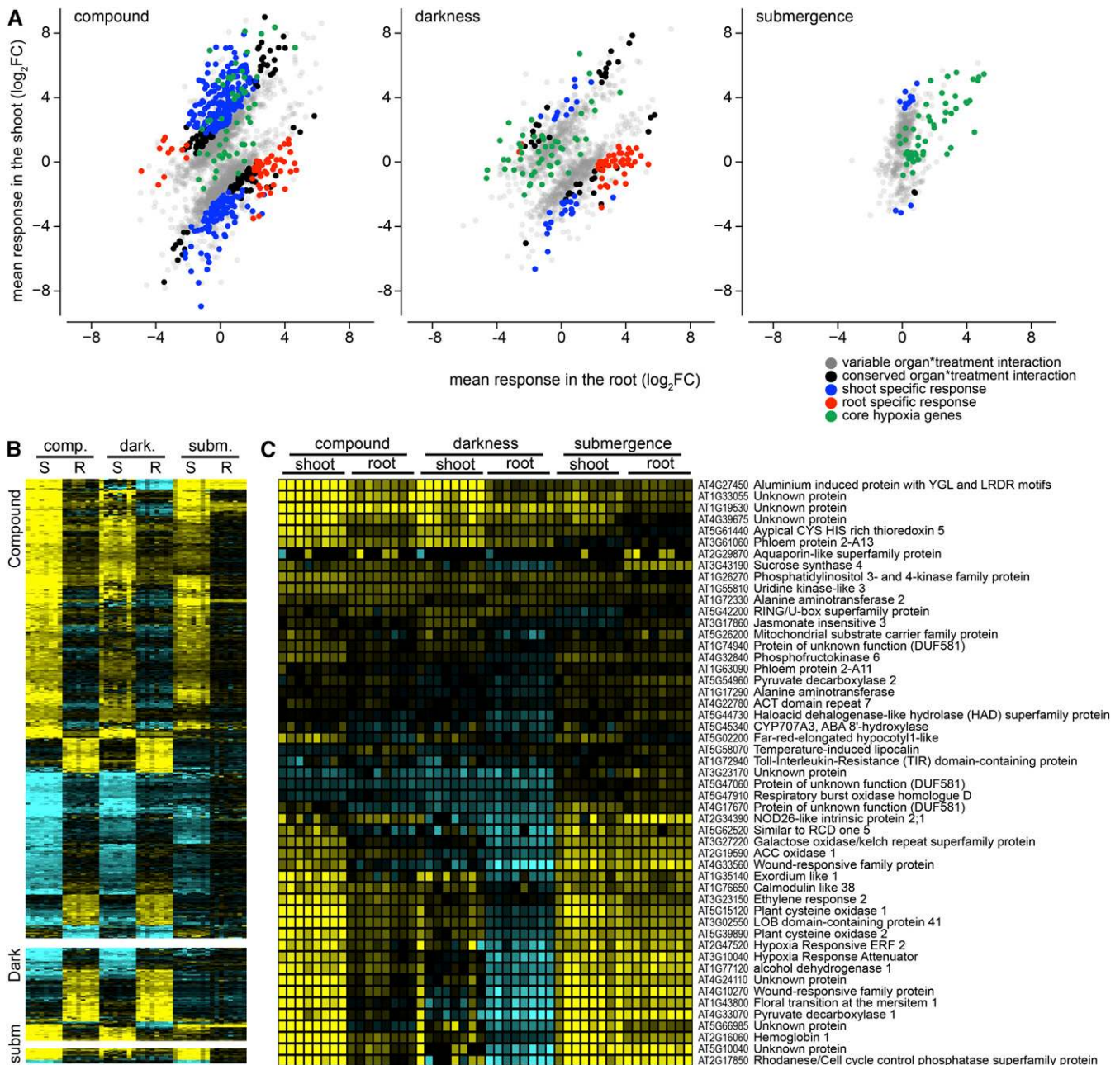


Figure 4. Organ-specific transcriptome reconfiguration and low-oxygen-responsive genes. **A**, Scatterplot showing the mean response of DEGs that show organ-dependent regulation by the treatment. Gray circles represent genes with a variable organ-specific response ($P_{organ*treatment, adj.} < 0.05$ in at least one accession). Black circles represent genes that show robust organ-specific behavior ($P_{organ*treatment, adj.} < 0.05$ in six, seven, or eight accessions). Blue circles represent shoot-specific genes that have a robust organ-treatment interaction (black) but also a robust treatment response in the shoot ($P_{adj.} < 0.05$ in six, seven, or eight accessions) but not a robust treatment response in the same direction in the root ($P_{adj.} < 0.05$ in six, seven, or eight accessions). Red circles represent root-specific genes that are similar in response to the shoot-specific genes. Green circles represent cell type-independent hypoxia-responsive genes (51 core hypoxia genes) as defined by Mustroph et al. (2009). **B**, Clustering of the organ-specific behavior for compound, darkness, and submergence responses identified in **A**. The $\log_2 FC$ of root (R)- and shoot (S)-specific genes (red and blue circles in **A**) is shown. The accessions are ordered from left to right for each organ and treatment: Cvi-0, Bay-0, Ita-0, Col-0 (*gl*), Kas-1, Lp2-6, Ws-2, and C24. Yellow indicates up-regulation and cyan indicates down-regulation. Genes shown and fold change values are given in Supplemental Data Set S1, Sheet H. **C**, $\log_2 FC$ of the 51 core hypoxia genes. The accessions are ordered as follows: Cvi-0, Bay-0, Ita-0, Col-0 (*gl*), Kas-1, Lp2-6, Ws-2, and C24 (left to right for each organ and treatment). Yellow indicates up-regulation and cyan indicates down-regulation.

isoform level corresponding to variations in mRNA splicing events. These events can include exon skipping, mutually exclusive (alternative) exon usage, and alternative donor and acceptor splice sites that can alter protein-coding and untranslated regions, all of which are generally termed AS. Another event is intron retention (IR), which involves the retention of introns in the mature mRNA. IR events that result in an open reading frame that is upstream of an intron junction typically target transcripts for nonsense-mediated decay and, therefore, are unstable mRNA isoforms (Kazan, 2003). We focused on splice site selection and IR variants similar to the method described by Chang et al. (2014) by characterizing the relative increase or decrease in specific variants between samples. More specifically, for each accession, we characterized AS and IR induced by the three treatments (compound, darkness, and submergence), and for each of the three conditions (AL, AD, and SD), we characterized the relative variant usage between the eight accessions.

Considerable levels of both IR and AS events were identified among the eight accessions, which was largely independent of the treatment (Supplemental Fig. S6, A and C). In total, 1,819 and 1,014 IR events were treatment independent ($\log_2 FC > 1$, $P_{adj.} < 0.01$) in the root and shoot, respectively (Supplemental Fig. S6B). For AS, 2,061 and 1,798 treatment-independent root and shoot events ($\log_2 FC > 1$, $P_{adj.} < 0.01$) were identified (Supplemental Fig. S6D). The consistency and strong overlap in AS and IR across the three conditions (AL, AD, and SD) indicated that these are robust differences between the accessions. However, with respect to the acclimative responses to darkness, compound, and submergence stress, the treatment-induced splicing events were of more interest (Fig. 5). While 1,214 and 2,122 genes with IR events ($\log_2 FC > 1$, $P_{adj.} < 0.01$ in at least one accession) were found in the root and shoot, the corresponding numbers for treatment-induced AS events ($\log_2 FC > 1$, $P_{adj.} < 0.01$ in at least one accession) were 210 (root) and 2,471 (shoot) genes. For both AS and IR events, the overlap between accessions was minimal (Fig. 5, B and D). However, the genes with conserved splicing behavior across the accessions were of interest as robust examples of darkness- and submergence-induced posttranscriptional regulation. Indeed, the 167 and 63 genes in the shoot and root that showed IR in five or more accessions showed consistent behavior across the accessions, and, depending on the gene, IR was favored either upon the stress condition (AD and SD) or under air light conditions (Supplemental Figs. S7 and S8).

Compared with IR, fewer treatment-dependent conserved AS events were identified, with 15 and 31 genes displaying AS in five or more accessions for roots and shoots, respectively (Fig. 6). For these genes, this additional aspect of transcriptome reconfiguration in response to compound, darkness, or submergence stress would not only affect mRNA stability, as is the case for IR, but potentially also could lead to altered protein function and localization or influence other

posttranscriptional processes such as translational efficiency. These regulatory processes would be in addition to the differences we already observed in the total transcript abundance of these genes between the treatments (Supplemental Fig. S9). To verify the validity of the observed AS patterns, independent real-time quantitative reverse transcription (qRT)-PCR analyses using Cvi-0 and C24 accessions as representatives were done. We tested six genes that, in addition to showing distinct AS patterns, also showed strong transcriptional regulation. All six genes tested confirmed the mRNA-seq-based evidence of AS (Fig. 7). This also revealed that AS began within a few hours of stress and persisted at elevated levels over 48 h of compound, darkness, and submergence treatments (Fig. 7). For most genes tested, the increase in splice variant isoform(s) occurred rapidly and then declined somewhat (e.g. *ROPGEF11* [AT1G52240]; Fig. 7). Several of the 46 genes with conserved AS events could have important roles in acclimation to the imposed stress.

For instance, in the root, *ROPGEF11* preferentially produced a short transcript over a longer transcript isoform under darkness and compound stress, with total transcript abundance elevated by both stresses (Figs. 6 and 7). The shorter isoform lacks the ROP nucleotide exchanger domain (PF03759), which for *ROPGEF11* is implicated in phytochrome interactions in the regulation of root development (Shin et al., 2010), and instead contains a dynein light chain domain (PF01221; Fig. 8A). Another interesting gene was *ARR1*, a cytokinin response regulator (Kieber and Schaller, 2014) that was darkness induced and accumulated an alternatively spliced variant in the shoot and root (Figs. 6 and 8B). Although AS of the pre-mRNA of *ARR1* results in transcript isoforms that encode two distinct proteins, both contain all known conserved domains of the receptor but differ in their C termini. The isoform variant of *ARR1* that is elevated in darkness also has a shorter and distinct 3' untranslated region, which could influence the interaction with RNA-binding proteins that alter mRNA stability or translation.

Among the genes displaying AS was a relatively large group of genes associated with metabolic functions (Fig. 6). Many of these were differentially regulated by either darkness or submergence. These included two Fru bisphosphate aldolases (*FBA1* and *FBA5*), a Suc 6-phosphate phosphorylase, and *GLUTAMATE DEHYDROGENASE2*. Also of relevance was *PEROXISOMAL NAD-MALATE DEHYDROGENASE2* (*PMDH2*), which is required for redox balance during fatty acid breakdown in the peroxisome (Pracharoenwattana et al., 2007). *PMDH2* AS upon darkness and submergence favored an enzyme form with increased activity (Fig. 8C). Of particular interest were the AS patterns of *PPDK* (AT4G15530) and *LKR/SDH* (AT4G33150). *PPDK* is a single-copy gene that is induced by low oxygen in a variety of species (Huang et al., 2008). Of the five *PPDK* transcript isoforms, the shortest transcript (AT4G15530.2) preferably and progressively accumulated upon darkness and submergence (Figs. 7 and 8D).

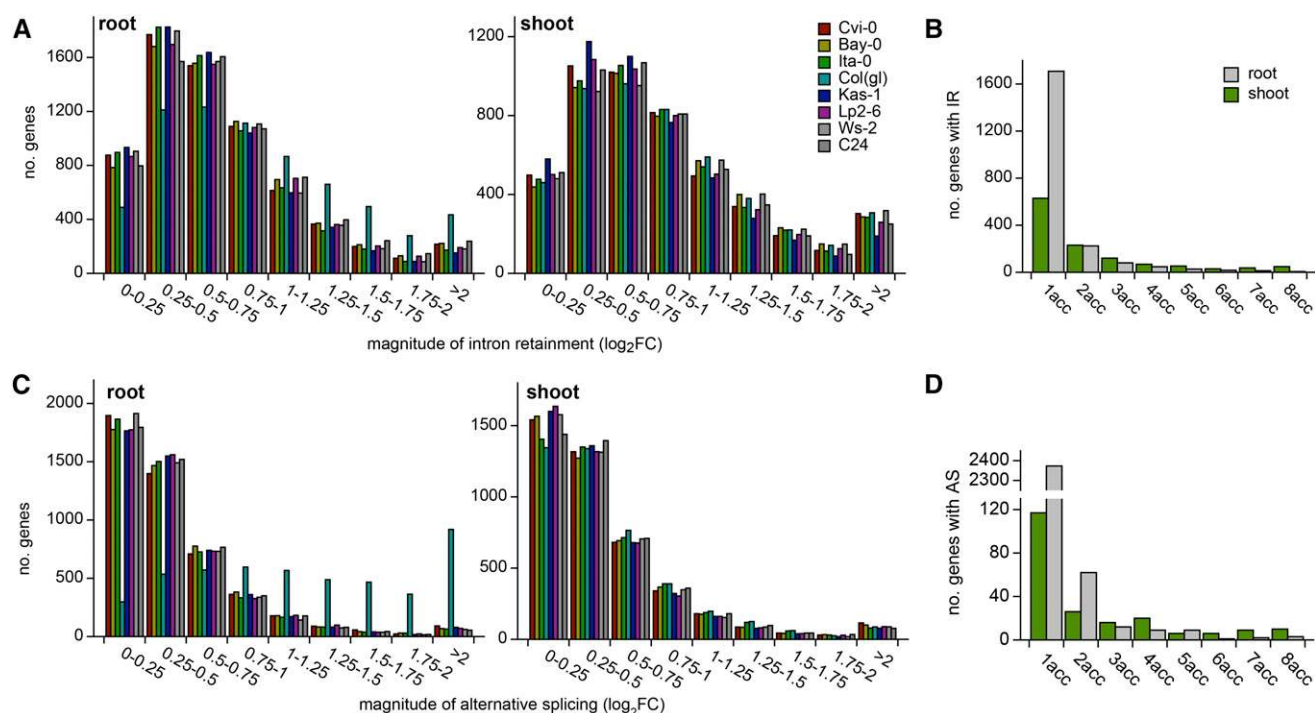


Figure 5. AS and IR upon compound, darkness, and submergence stress. A, Histograms show the magnitude of IR (calculated as the maximum difference in IR) upon the treatments for each accession. B, Number of genes in the shoot (green bars) and root (gray bars) that show IR upon treatment (compound, dark, and submergence), and their overlap between accessions [$\log_2(\text{obs}/\text{exp}) > 1$ and $P_{\text{adj.}} < 0.01$]. C, Histograms show the magnitude of AS (calculated as the maximum difference in AS) upon the treatments for each accession. D, Number of genes in the shoot (green bars) and root (gray bars) that are alternatively spliced upon treatment (compound, dark, and submergence), and their overlap between accessions [$\log_2(\text{obs}/\text{exp}) > 1$ and $P_{\text{adj.}} < 0.01$].

This transcript encodes the cytosol-localized form of PPDK (Parsley and Hibberd, 2006) that is suggested to be important during amino acid remobilization and senescence (Taylor et al., 2010) and for gluconeogenesis (Eastmond et al., 2015). Interestingly, several other genes involved in gluconeogenesis were quantitatively up-regulated or down-regulated in response to the compound and darkness treatments (Supplemental Fig. S10). Of these, only *PPDK* showed pronounced up-regulation across accessions under submergence.

LKR/SDH (AT4G33150) encodes a bifunctional enzyme catalyzing the first two steps of Lys catabolism. While the LKR component of the protein works in the Lys catalytic direction, the SDH component has bidirectional enzymatic activity (Zhu et al., 2002). Besides being strongly up-regulated by darkness and compound stress in roots and shoots (Supplemental Fig. S9), AS of *LKR/SDH* was evident in the root (Figs. 6, 7, and 8E), with the longer transcript being favored under both conditions (Fig. 7E). The long transcript results in a protein with both LKR and SDH activity, whereas the short transcript only has SDH activity (Zhu et al., 2002).

In the shoot, a relatively large amount of AS occurred in transcripts related to photorespiration (*GLYCERATE KINASE* and *GLYCOLATE OXIDASE1*), light capture (*PHOTOSYSTEM 1 LIGHT HARVESTING COMPLEX GENE1*, a putative cytochrome *b_f* complex subunit, and

NONPHOTOCHEMICAL QUENCHING1 [*NPQ1*] and *NPQ4*), CO₂ sensing (*BETA-CARBONIC ANHYDRASE1* [*BCA1*] and *BCA4*), and plastid development (F-box family protein, *PLASTID REDOX INSENSITIVE2* [*PRIN2*], and *TRANSLOCON AT THE OUTER ENVELOPE MEMBRANE OF CHLOROPLAST*). These AS variants do not necessarily lead to distinctions in the encoded protein but modify untranslated regions of the mRNA (Fig. 8, F and G) and, hence, could influence other posttranscriptional processes. Intriguingly, both *BCA1* and *BCA4* displayed differences in the 5' untranslated region between the treatments (Fig. 8, H and I). The isoforms preferentially accumulating in darkness and submergence encode N-terminally truncated proteins that retain enzymatic activity but lack the sequences responsible for specific subcellular targeting (*BCA1* to the chloroplast and *BCA4* to the plasma membrane; Fabre et al., 2007). Altogether, these data demonstrate that AS can serve as a posttranscriptional control point that impacts the accumulation, location, and activity of a number of proteins that regulate carbon flux.

Natural Variation in Submergence Tolerance Is Associated with Relatively Minor Transcriptomic Differences in a Group of Putative Tolerance Genes

A previous study that used an identical experimental setup showed considerable variation in the tolerance to

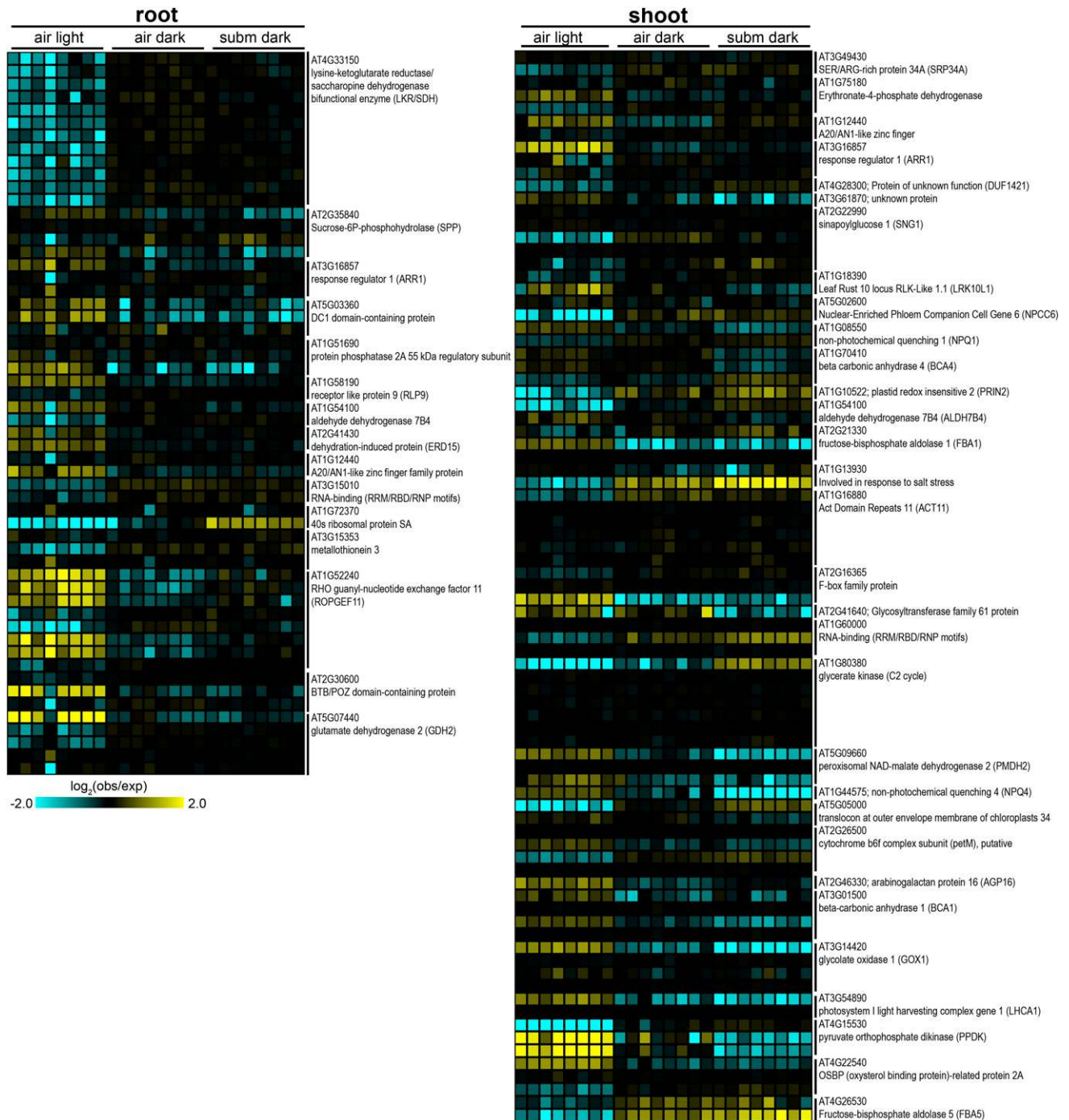


Figure 6. The conserved compound-, darkness-, and submergence-induced AS. For each variant-identifying gene region (VIGR), the deviation from the expected read counts if no change in variant usage upon treatment would take place [$\log_2(\text{obs/exp})$] is shown for roots and shoots. Yellow indicates more, and cyan fewer, reads than expected for a specific VIGR. All genes that are alternatively spliced [$\log_2(\text{obs/exp}) > 1$ and $P_{\text{adj.}} < 0.01$] in five or more genotypes are shown. For each condition, the genotypes are ordered from left to right: Cvi-0, Bay-0, Ita-0, Col-0 (*gl*), Kas-1, Lp2-6, Ws-2, and C24.

complete submergence in the dark (compound stress) among 86 *Arabidopsis* accessions (Vashisht et al., 2011). This variation could not be ascribed to differences in anatomy, decline in organ oxygen content, or initial carbon resources. Based on that study, three accessions

profiled here were classified as submergence sensitive (Cvi-0, Bay-0, and Ita-0) and three as tolerant (Lp2-6, Ws-2, and C24). The tolerant accessions also performed better when their survival under submerged conditions (SD) was compared with their survival under darkness

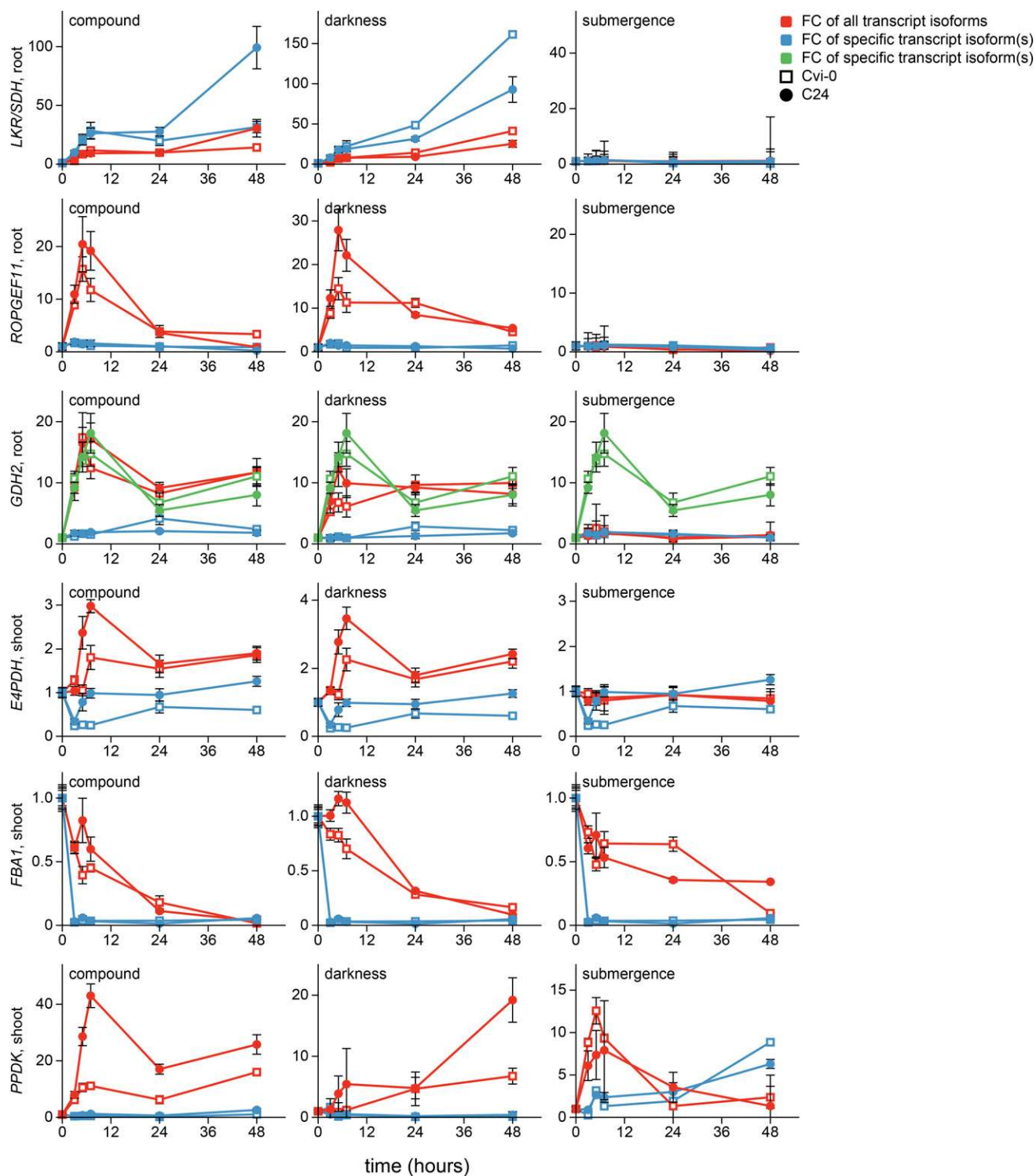


Figure 7. qRT-PCR validation of a selection of genes alternatively spliced upon compound, darkness, and submergence. Fold change of transcript abundance is shown in accessions Cvi-0 and C24 upon compound, darkness, and submergence of six genes that were identified as alternatively spliced upon the treatment in a conserved manner across accessions. Primers were used that either amplified all transcript variants (red lines) or selectively amplified only specific variants (blue and green lines). Root or shoot tissue was analyzed depending on the organ in which AS was identified. Details for each gene are as follows: *LYSINE-KETOGLUTARATE REDUCTASE/SACCHAROPINE DEHYDROGENASE* (AT4G33150, *LKR/SDH*, root), the blue line represents AT4G33150.1 and AT4G33150.2; *RHO GUANYL-NUCLEOTIDE EXCHANGE FACTOR11* (AT1G52240, *ROPGEF11*, root), the blue line represents AT1G52240.1; *GLUTAMATE DEHYDROGENASE2* (AT5G07440, *GDH2*, root), the blue line

Downloaded from https://academic.oup.com/plphys/article/172/2/668/6115920 by guest on 21 August 2022

(AD; submergence stress). Based on that prior study, genes that responded differently to compound and submergence stress were identified by comparing the tolerant and sensitive accessions ($P_{\text{tolerance} \times \text{treatment, adj.}} < 0.05$; Supplemental Data Set S1, Sheet K). In this way, 33 and five potential tolerance genes were identified in the shoot for compound and submergence stress, respectively (Fig. 9A; Supplemental Data Set S1, Sheet K). A larger number of potential tolerance genes were identified for the root (47 compound and 43 submergence). Although this relatively large number of potential tolerance genes could be responsible for differential tolerance among these accessions, the magnitude of the difference was not always large (Fig. 9B).

Interesting shoot potential tolerance genes with a stronger overall increase in expression in tolerant genotypes included the inorganic pyrophosphate (PPi)-utilizing and gluconeogenic enzyme PPDK (AT4G15530), a gene encoding a natural antisense RNA (AT4G20362), and a RAB GTPase homolog (AT4G20360). Also predominantly up-regulated in tolerant genotypes was plant *DEFENSIN1.2b* (AT2G26020). Additionally, the shoot potential tolerance genes included several growth- and cell wall-associated genes such as *XYLOGLUCAN ENDOTRANSGLUCOSYLASE/HYDROLASES4*, an auxin-responsive GH3 family protein, and *EXPANSIN A16*, which were more induced in the sensitive accessions (Supplemental Data Set S1, Sheet K). This suggested a more conserved growth response in the tolerant accessions in our treatment conditions. To assess whether this was indeed true, petiole elongation rates of a sensitive (Cvi-0) and tolerant (C24) accession were measured as a marker for shoot growth (Supplemental Fig. S11). The tolerant C24 had a greater reduction in petiole elongation rates (relative to AL) compared with Cvi-0 in both light and dark submerged conditions. In the dark, Cvi-0 petiole elongation rates were similar to those of control plants. In contrast, in C24, petiole elongation rates were reduced to less than 33% of control (AL) rates.

The potential tolerance genes from the root were of a different nature compared with the shoot, and no overlap in gene composition was found between the two organs. For instance, *FERRIC REDUCTION OXIDASE4* (*FRO4*) and *FRO5* (AT5G23980 and AT5G23990), which play important roles in the uptake of iron and copper from the soil (Bernal et al., 2012; Jain et al., 2014), were identified. Additionally, a vacuolar iron transporter and a metal transporter (*VACUOLAR IRON TRANSPORTER-LIKE5* [AT3G25190] and *ZRT/IRT-LIKE PROTEIN2* [AT5G59520]) were classified as potential tolerance genes. All of these genes had

stronger down-regulation in the tolerant accessions, especially upon submergence. Another root potential tolerance gene, *LOW PHOSPHATE ROOT1* (AT1G23010), is involved in sensing and signaling of low inorganic phosphate availability in the root in an iron-dependent manner (Svistoonoff et al., 2007; Müller et al., 2015) and was up-regulated in the sensitive and down-regulated in the tolerant accessions (Supplemental Data Set S1, Sheet K).

Interestingly, several of the potential tolerance genes identified here have been identified previously as commonly hypoxia regulated throughout the plant kingdom (Mustroph et al., 2010). This was especially the case in the root, with tolerance group-dependent regulation upon the compound stress for *HYPOXIA UNKNOWN PROTEIN37* (AT2G41730), *SIMILAR TO RCD ONE5* (*SRO5*; AT5G62520), an unknown protein (AT3G23170), and *CALMODULIN-LIKE38* (AT1G76650), recently shown to be a calcium-regulated cytosolic RNA-binding protein (Lokdarshi et al., 2016). A close homolog of *SRO5*, namely *SRO4* (AT3G47720), also was identified as a tolerance gene in the root. For the shoot compound stress, this category of genes included *PPDK* (AT4G15530) and *PYRUVATE DECARBOXYLASE1* (AT4G33070).

DISCUSSION

Anatomical and physiological features contribute little toward the large variation in the tolerance to darkness and submergence observed in Arabidopsis accessions (Vashisht et al., 2011). For this reason, the short-term transcriptomic acclimation was investigated in a selection of eight accessions under highly controlled conditions that closely mimic natural flooding events in the field. Furthermore, the experimental design made it possible to disentangle the effects of darkness from the responses caused by reduced gas diffusion (i.e. oxygen, CO₂, and ethylene) in the underwater environment. This allowed us to identify conserved processes in relation to the naturally occurring stress while simultaneously identifying accession- and tolerance-specific processes. The systematic comparison of the shoot and root transcriptomic adjustments of eight accessions to flooding and starvation stress revealed robust conservation in a response, which encompasses specific transcript isoform production but also contained subtle and possibly significant distinctions between flooding-tolerant and intolerant accessions. Our results emphasize that understanding plant adaptation to flooding requires consideration of its compound nature, which often includes reduction in light or even complete

Figure 7. (Continued.)

represents AT5G07440.1 and AT5G07440.2 and the green line represents AT5G07440.1 and AT5G07440.3; *ERYTHRONATE-4-PHOSPHATE DEHYDROGENASE* (AT1G75180, *E4PDH*, shoot), the blue line represents AT1G75180.2 and AT1G75180.3; *FRUCTOSE-BISPHOSPHATE ALDOLASE1* (AT2G21330, *FBA1*, shoot), the blue line is specific for AT2G21330.2; *PYRUVATE ORTHOPHOSPHATE DIKINASE* (AT4G15530, *PPDK*, shoot), the blue line represents all transcripts, excluding AT4G15530.2.

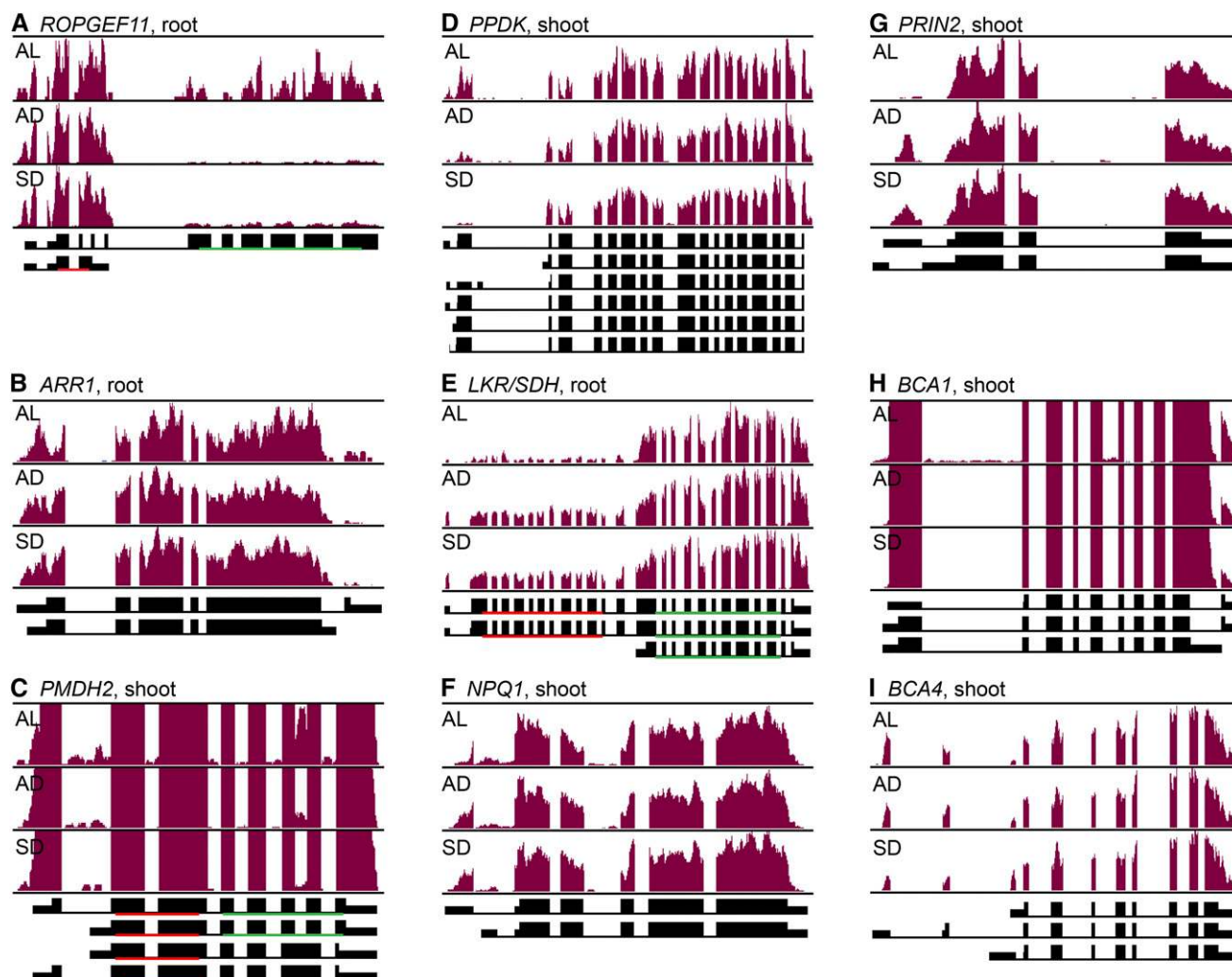


Figure 8. Coverage plots of a selection of genes that are alternatively spliced in response to the imposed treatments. Coverage plots were normalized to the maximum read depth or a percentage of maximum read depth. Gene models (introns, line; exons, thick box; untranslated region, thin box) are shown below ordered from the first model (0.1) onward and are depicted from left to right in the 5' to 3' direction. Red and green lines indicate the locations of intact protein domains specific to certain transcript isoforms. A, *ROPGEF11*, AT1G52240, in Bay-0. Red domain, dynein light chain domain (PF01221); green domain, PRONE (PF03759). B, *ARR1*, *ARABIDOPSIS RESPONSE REGULATOR1*, AT3G16857, in Bay-0. C, *PMDH2*, *PEROXISOMAL NAD-MALATE DEHYDROGENASE2*, AT5G09660, in Bay-0. Red domain, NAD-binding domain; green domain, malate dehydrogenase α/β C-terminal domain. D, *PPDK*, AT4G15530, in Bay-0. E, *LKR/SDH*, AT4G33150, in Bay-0. Red domain, LKR activity; green domain, SDH activity (Zhu et al., 2002). F, *NPQ1*, *NONPHOTOCHEMICAL QUENCHING1*, AT1G08550, in Bay-0. G, *PRIN2*, *PLASTID REDOX INSENSITIVE2*, AT1G10522, in Bay-0. H and I, *BCA1* and *BCA4*, AT3G01500 and AT1G70410, in Lp2-6.

darkness in combination with a severe reduction of gas exchange.

Alternative Metabolic Reserve Mobilization as a Coordinated Transcriptional Response to Darkness and Submergence

Darkness and submergence both cause similar physiological changes in affected plants, including carbohydrate depletion, utilization of alternative carbon sources, and chlorophyll degradation. However,

Arabidopsis has an amazing capacity to buffer its metabolism to unexpected darkness (Graf et al., 2010). An unexpected early night leads to appropriate reductions in the rate of starch breakdown. This adjustment allows the available carbohydrate reserves to last throughout the longer than expected night and thus prevents starvation-related transcriptional responses. However, our data set revealed transcriptome reconfigurations typical of starvation responses already within 4 h. This suggests that imposing darkness or submergence stress during approximately the first half of the light period

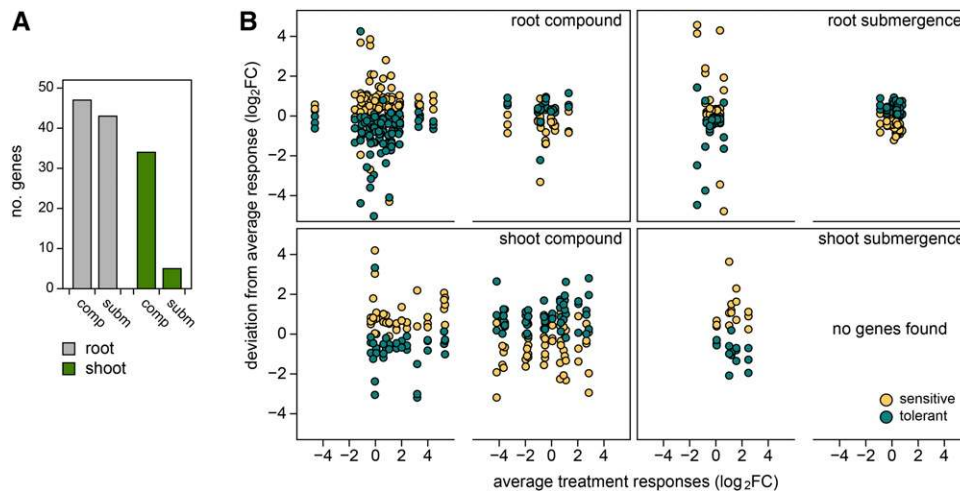


Figure 9. Flooding tolerance-dependent compound, darkness, and submergence responses. A, Number of DEGs in the shoot and root where the treatment response depends on the tolerance group ($P_{\text{tolerance} \times \text{treatment, adj.}} < 0.05$). Flooding tolerance classification is based on Vashisht et al. (2011). Sensitive accessions are Cvi-0, Bay-0, and Ita-0, and tolerant accessions are Lp2-6, Ws-2, and C24. B, Tolerance-specific DEGs (from A) that show distinct responses between the flooding-tolerant (teal circles) and sensitive (yellow circles) accessions and their deviation from the average treatment response (for root and shoot compound and submergence treatments). Within each group, left graphs show DEGs with fold change higher in the tolerant accessions and right graphs show DEGs with fold change higher in the sensitive accessions.

under short-day conditions is taxing on the buffering capacity of *Arabidopsis*. The metabolic buffering capacity has been shown to require the circadian clock and targets starch breakdown (Graf et al., 2010). Consistently, in our analysis, starch breakdown and biosynthesis were predominantly down-regulated upon darkness, an effect that was even stronger when coupled with submergence. However, while the clock and circadian machinery also were affected by darkness, there was no additional effect of submergence, in line with the large contribution of light cues in entraining the circadian rhythm (Hsu and Harmer, 2014).

Instead of starch, the transcriptional activation of fatty acid and amino acid breakdown was observed, indicating the occurrence of autophagy (intracellular degradation and recycling of cellular components). *Arabidopsis* mutants defective in autophagy are highly sensitive to submergence (Chen et al., 2015). Several of these genes involved in fatty acid and amino acid breakdown are crucial to maintain energy status and performance during stress conditions or in non-photosynthetic developmental stages. This was shown in mutant studies on *LKR/SDH* (Lys breakdown) and *PMDH2* (fatty acid β -oxidation) in heterotrophic germinating seeds (Pracharoenwattana et al., 2007; Angelovici et al., 2011). Interestingly, for both these genes, specific transcript isoforms were preferentially induced upon compound, darkness, and submergence stress. For *LKR/SDH*, the preferentially induced longer transcript favors Lys breakdown (Tang et al., 2002), and for *PMDH2*, isoforms with the intact enzymatic domain preferentially accumulated, suggesting increased enzymatic activity upon the imposed stresses. Several other genes encoding key metabolic enzymes of the

amino acid and fatty acid breakdown pathways displayed AS upon compound, darkness, and submergence (Supplemental Fig. S12). This suggests that AS provides an additional layer of regulation that could have a significant impact on metabolite fluxes during these stress conditions.

A strong up-regulation of transcripts of glyoxylate pathway enzymes also was observed. The glyoxylate pathway shortcuts a part of the tricarboxylic acid cycle (from isocitrate to succinate), thereby preventing the loss of two CO_2 molecules and thus preserving fixed carbon. This suggests that protein and fatty acid breakdown is not necessarily being utilized in respiration and energy production but also is used for sugar biosynthesis. The activation of key steps of the gluconeogenic pathway, involving *PEP CARBOXYKINASE* (*PCK*) and *PPDK*, upon compound, darkness, and submergence further points toward the utilization and mobilization of alternative carbon resources (Supplemental Fig. S12). *PPDK* regulation was of special interest since the cytosolic transcript isoform that was preferentially up-regulated has been shown to increase nitrogen mobilization when overexpressed (Taylor et al., 2010). Furthermore, *PPDK* was more strongly up-regulated upon compound stress in the tolerant accession C24 than the sensitive Cvi-0, a pattern that persisted over time (Fig. 7). Besides their function in C4 photosynthesis, *PCK* and *PPDK* have been studied primarily in the context of their gluconeogenic role in reserve mobilization in germinating seeds (Penfield et al., 2004; Delgado-Alvarado et al., 2007; Malone et al., 2007; Eastmond et al., 2015) and around vein tissue, where they also display high activity (Hibberd and Quick, 2002; Brown et al., 2010).

Furthermore, *PPDK* and *PCK* are up-regulated in submerged *Rumex acetosa* (van Veen et al., 2013), anoxic rice coleoptiles (Narsai et al., 2009), and waterlogged Arabidopsis roots (Hsu et al., 2011).

In line with previously identified roles and functions, we hypothesize that under compound, darkness, and submergence stress, the enzymes *PCK* and *PPDK* could occupy a key function in fueling starving plant organs with reserves alternative to starch, possibly by redirecting energy-rich metabolites from source leaves to sink meristems and roots. An additional adaptive benefit of utilizing alternative resources to starch is that the maintenance and upkeep associated with high protein levels and organelles (Amthor, 2000) can be minimized. Thus, sacrificing older leaves, minimizing the requirements of young leaves, and concentrating resources in the meristems might provide a useful strategy to persist under adverse flooded conditions.

A common observation in studies profiling metabolic changes upon flooding is an increase in the levels of certain amino acids. This has been documented, for instance, in submerged rice shoots (Barding et al., 2013), anoxic rice coleoptiles (Narsai et al., 2009), and waterlogged poplar (*Populus* spp.) and *Lotus japonicus* (Kreuzwieser et al., 2009; Rocha et al., 2010). Indeed, in senescing leaves, increased protein breakdown and amino acid catabolism coincide with increased amino acid content (Watanabe et al., 2013; Hildebrandt et al., 2015). Similarly, in petioles of submerged *R. acetosa* plants, a large increase in free ammonia was observed upon submergence, suggesting an increased amino acid breakdown (van Veen et al., 2013). Further metabolic evidence for amino acid catabolism comes from Arabidopsis mutants defective in energy starvation signaling. In these lines, a similar suite of catabolic and gluconeogenic genes were regulated as observed here, including *PPDK*, and a subsequent altered metabolic profile was observed (Hartmann et al., 2015). However, it is difficult to discern metabolic fluxes from transcriptomic and metabolomic data except when start or end products of specific routes are quantified. Indeed, Rocha et al. (2010) and Antonio et al. (2016) provide a model based on isotope flux determination, specific to low oxygen availability induced by waterlogging, where the intertwining of nitrogen metabolism and the tricarboxylic acid cycle potentially doubles ATP production relative to glycolysis alone when the mitochondrial electron transport chain is compromised. This requires pyruvate to be funneled to Ala, to prevent pyruvate-induced respiration, blocking of the tricarboxylic acid cycle at succinate dehydrogenase (also down-regulated in our study; Supplemental Fig. S12), and activation of the γ -amino butyric acid shunt. These, however, could be fundamentally different processes from what is observed under our experimental conditions, given that the bulk of the transcriptomic changes we observed occurred in response to darkness in air-grown plants, where the advantages of these adaptations to low oxygen would be less apparent.

Although we assign a significant role to *PPDK* in resource mobilization, its relevance during hypoxic conditions has been attributed previously to its role in the low-oxygen-induced switch to PPI-dependent glycolysis (Huang et al., 2008; Mustroph et al., 2014b). The primary advantage of PPI-utilizing enzymes such as *PPDK* is the conservation of ATPs and the yield of additional ATPs for each sugar molecule going through glycolysis. This could be essential for survival during low-oxygen conditions when the electron transport chain, which provides the bulk of ATP, is hampered. However, the activation of *PPDK* already under darkness strongly favors a role in gluconeogenesis, since under these conditions the ATP gain is almost negligible. Although PPI-utilizing enzymes do provide a more energetically favorable route during anaerobic metabolism, whether these pathways are preferred during low-oxygen conditions is now under scrutiny. Analyses of Suc synthase mutants under hypoxic conditions suggest that, despite hampered performance under flooding stress, a major portion of the carbon provided for glycolysis is still generated by the ATP-dependent invertase and not via the PPI-linked Suc synthase route, at least in Arabidopsis (Santaniello et al., 2014). In the context of the role of *PPDK* as well, a reassessment might be required for its precise role during hypoxic glycolysis.

The observation that, upon submergence, the shoot shows an amplification of the darkness response underscores the knowledge that plants tightly adjust their metabolism to suit their environmental conditions. Additionally, we observed that the transcriptional changes identified here are typical of carbon and energy starvation, which requires resource mobilization. In addition to this, the differential regulation of translation is another regulatory control point under hypoxia and in darkness (Branco-Price et al., 2008; Pal et al., 2013; Juntawong et al., 2014). Our studies also suggest that AS might play an important role in this response as an additional layer of regulation in the coordinated mobilization of existing and alternative reserves to endure starvation conditions and prolong underwater survival (Supplemental Fig. S10).

Organ-Specific Transcriptome Reconfiguration and Oxygen-Dependent Responses

Previous studies have shown that, following low-oxygen stress and submergence, the root and shoot transcriptomes are reconfigured in a distinct manner underscoring variation between these organs in cues and protective mechanisms (Ellis et al., 1999; Mustroph et al., 2009, 2014a; Lee et al., 2011). The differences between root and shoot in their transcriptome responses to darkness and submergence signals can be attributed to several factors, including the autotrophic and heterotrophic natures of the shoot and root, respectively, different cellular identities and composition, distinct physiological functions, and varying oxygen profiles.

Endogenous oxygen levels are determined primarily by a balance between the internal production/consumption and the rate of inward diffusion from the surrounding environment (soil, air, or water). In *Arabidopsis* roots, oxygen levels drop from 6% to 0% and in the petiole from 17% to 6% pO₂ KPa (Lee et al., 2011) within 3 h (oxygen levels in the lamina are unknown). The transcriptomic profiling of both organs using mRNAseq allowed for a detailed investigation of organ-specific responses to darkness, submergence, and the role of oxygen herein.

The large-scale differences between the organs were typified by a higher number of DEGs and stronger gene expression fold changes in the shoot than in the root. A possible explanation for the greater responsiveness of the shoot is that roots continuously habituate a dark environment under control (AL) conditions, meaning that the transition to dark treatment would have had a relatively smaller impact. The fact that *Arabidopsis* roots are nonphotosynthetic and constitutively a sink also may contribute to their less dramatic responsiveness. More striking, however, was the lack of an amplification of the darkness responses in the compound transcriptome behavior in the root. This also could reflect the existing sink-source relationship between the root and shoots: roots typically dependent on the shoot for carbon resources were already maximally starved after the dark treatment, whereas the shoot had more reserves to buffer the response.

Despite the fewer transcriptional changes observed in the root, several processes were identified as root specific. Plants have several sensing and signaling mechanisms to detect changes in redox and maintain redox homeostasis, which is important in all aspects of plant growth and development. Interestingly, genes of this category were prevalent among the root-specific genes such as thioredoxins and rubredoxin. Furthermore, many photosynthesis-related genes were among the root-specific genes (e.g. PSI and PSII proteins). The increased expression of these genes and several other chloroplast-associated genes in the roots indicates the presence of chloroplasts in this organ, likely in the cortex (Dinneny et al., 2008). While root greening has been described before, it is known to occur only in the presence of a light signal (Usami et al., 2004; Kobayashi et al., 2012). Elevated transcripts encoding photosynthesis-chloroplast-associated proteins in roots were reported previously in hypoxic/flooded seedlings of *Arabidopsis* and *Rorippa* spp. (Chang et al., 2012; Sasidharan et al., 2013). In contrast to this work, the roots in these studies were at some point exposed to light signals. Sugar starvation and salt stress also are reported to induce photosynthesis-associated genes in roots (Sheen, 1990; Baena-González et al., 2007; Dinneny et al., 2008). It has been speculated that this might be triggered by reactive oxygen species (ROS) generated during the stress and with a potential role in ROS amelioration (Dinneny et al., 2008). The relevance of the expression of these genes in a root-specific manner upon darkness and compound stress in the absence of a

light signal remains intriguing. The regulation of ROS production is likely a relevant function in stressed roots. However, whether this is the case here, and what the underlying mechanism is, remain to be determined.

Unlike the root, the shoot responded differently to darkness and submergence. Shoot-specific genes up-regulated by these conditions across the accessions were associated with growth, senescence, and oxidative stress, all elements of the underwater response. Although there was an up-regulation of transcripts of genes associated with growth and growth-associated hormonal signaling (GA and ABA) in the shoot, the petiole elongation response to dark and compound stress was varied across accessions (Supplemental Fig. S11; Vashisht et al., 2011). Considering that whole shoots were sampled here, the involvement of these shoot-specific genes in mediating changes in leaf expansion or perhaps hyponasty cannot be ruled out. Nevertheless, the shoot core gene set reflects growth regulation and extensive regulation of cell wall-modifying proteins and growth regulatory hormones. This likely is reflective of specific growth strategies that are an important mechanism to deal with both flooding (van Veen et al., 2014b) and low-light conditions (Gommers et al., 2013).

Interestingly, among the compound shoot-specific genes was a subset of core hypoxia genes. Although previous studies have established their cell type-independent hypoxia up-regulation, the shoot-specific regulation here was not surprising (Mustroph et al., 2009). Oxygen measurements on soil-grown plants in an identical setup revealed that, despite being in well-aerated soils, these soil-grown roots were already hypoxic (approximately 6% pO₂ KPa). Considering the already hypoxic conditions of roots under control conditions, it can be speculated that the constitutive expression of these genes is associated with acclimation to hypoxic conditions. Unlike seedlings grown on vertical agar plates that experience a normoxic-to-hypoxic transition, in our system, submerged roots transition from hypoxic to severely hypoxic conditions (Lee et al., 2011). Interestingly, it has been shown that low oxygen in the root tip only is sufficient to activate low-oxygen-responsive genes throughout the entire root (Mugnai et al., 2012). In active meristems, hypoxia is a common event during periods of high activity (van Dongen and Licausi, 2015). Interestingly, darkness caused a significant repression of the core hypoxia genes in the root. This suggests that, although similar physiological responses are triggered during submergence and darkness, associated with starvation conditions, transcriptomic responses are prioritized to adapt to starvation in the presence of oxygen. The core hypoxia signature including the inefficient fermentative mode of energy generation would then be a wasteful mode of energy generation under carbon-limiting conditions.

Clearly, in the final compound response, the behavior in response to darkness largely determines the difference between the shoot and root for these cell type-independent hypoxia-responsive genes (Fig. 4C).

However, overall, a shift to severe or mild low-oxygen levels did not lead to a different response when the effects of darkness were disregarded, and only submergence-induced hypoxia was considered. Even the magnitude of the core hypoxia gene up-regulation was similar for shoots and roots (Fig. 4, A and C). Remarkably, these distinct transcriptomic reconfigurations of the shoot and root systems were highly conserved across the eight accessions of *Arabidopsis*.

Natural Variation in Submergence Tolerance

Natural variation in stress responses can be exploited to identify molecular processes and components that regulate stress responses in a differential way and, therefore, determine tolerance. Previous studies established significant variations in flooding tolerance of six accessions used in this study at the level of whole-plant survival (Vashisht et al., 2011). This allowed us to classify the accessions into two tolerance groups and correlatively identify potential tolerance genes based on altered transcript accumulation or distinctions in AS. Interestingly, the potential tolerance genes identified in the root had no overlap with those from the shoot, further underscoring the distinct physiological states and functions of these two organs. Despite the lack of overlap between root and shoot potential tolerance genes, both included members of the core hypoxia-responsive gene set.

Interesting shoot potential tolerance genes that have not been implicated previously in flooding survival included the gluconeogenic enzyme PPDK, which was highly up-regulated in the tolerant accessions. Targeted qRT-PCR analyses confirmed this trend over a 48-h period (Fig. 7) and revealed a much stronger up-regulation in the tolerant (C24) accession. Previous studies have suggested a role for the PPi-utilizing PPDK in mobilizing protein stores (Huang et al., 2008) and in facilitating nitrogen remobilization in senescing leaves (Taylor et al., 2010). Furthermore, it has a key position in a metabolic network we identified as being important during starvation and submergence (Supplemental Fig. S12). It further stresses the importance of efficient alternative reserve mobilization during energy-limiting conditions. Future biochemical and metabolic studies are necessary to determine if up-regulation of a cytosolic PPDK enhances the utilization of noncarbohydrate stores to enhance energy production and long-term survival.

Another interesting shoot-specific potential tolerance gene was an antisense to a RAB GTPase homolog (AT4G20360) with organellar translation elongation factor activity. Previous studies have shown that *Arabidopsis* seedlings exposed to hypoxia drastically limit translation as a means to curb energy expenditure (Branco-Price et al., 2008; Juntawong et al., 2014; Sorenson and Bailey-Serres, 2014). The up-regulation of this antisense RNA in tolerant accessions could serve to limit elongation factor-Tu synthesis, thereby

limiting overall levels of plastid or mitochondrial mRNA translation.

Several shoot potential tolerance genes that were induced only in the sensitive accessions had functions in growth and cell wall remodeling, implying more dampened growth responses in the tolerant genotypes. Consistently, we found that petiole elongation rates were significantly lower in submerged plants (relative to control [AL]-grown plants) of a tolerant accession (C24). In contrast, a sensitive accession (Cvi-0) maintained control petiole growth rates under compound stress (SD) conditions (Supplemental Fig. S11). Taken together, this suggests that tolerance in *Arabidopsis* can be attributed to a conservative mode of energy utilization and efficient carbohydrate management resulting in prolonged underwater survival.

Tolerance is a complex phenomenon, especially in the case of a compound stress like flooding. Several aspects come into play, such as the environmental conditions and the physiological state of the plant before, during, and after submergence. Our data suggest that tolerant *Arabidopsis* accessions have restricted shoot growth and exhibit conservative and alternative resource utilization, involving specific stress-induced metabolic readjustments. This is likely an important factor influencing tolerance in the shoot, while in the roots, tolerance appears to involve genes related to hypoxia and development. This suggests that, to achieve tolerance, different alterations may be required in the root and shoot.

The tolerance of starvation stress is another factor that interacts with low-oxygen stress to influence the final outcome of tolerance. As observed here, some accessions (i.e. Ws-2 and Cvi-0) showed largely overlapping dark and submergence transcriptomes. This suggests that the tolerance of Ws-2 could be partly due to its ability to withstand starvation stress. Similarly, the sensitivity of Cvi-0 is likely linked to its poor performance under dark conditions (Vashisht et al., 2011). Accordingly, Cvi-0 petiole growth rates in the dark (AD) equaled control (AL) rates. This would likely result in a faster depletion of existing energy and carbohydrate reserves under stress conditions and hasten plant demise.

CONCLUSION

The current upsurge in the number of global flooding events underscores the importance of understanding tolerance mechanisms and plant responses to flooding stress. Knowledge of the basis of variation in stress tolerance also is critical for developing more stress-resistant crops for environments experiencing unexpected floods. This work details transcript abundance and AS alterations in soil-grown vegetative-stage *Arabidopsis* rosettes that were surprisingly conserved across a set of eight diverse genotypic backgrounds. Contrasting with this conservation was the distinct transcriptomic reconfiguration of the shoot and root

across the accessions, reflecting each organ's anatomical and physiological identity and highlighting unique metabolic and developmental plasticity as a result of the stress. We showed that alternative selection of splice sites provides an additional layer of molecular regulation to fine-tune the response to flooding and starvation stress. Our study also reveals that tolerance in *Arabidopsis* is related to the ability to restrict shoot growth and exhibit conservative and alternative resource utilization involving specific stress-induced metabolic readjustments.

MATERIALS AND METHODS

Plant Material and Growth Conditions

Seeds of the studied *Arabidopsis* (*Arabidopsis thaliana*) accessions (Bay-0, N22633; C24, N22620; Col-0 [g11], N3879; Cvi-0, N22614; Ita-0, N1244; Kas1, N22638; Lp2-6, N22595; and Ws-2, N1601) were obtained from the Nottingham Arabidopsis Stock Centre. They were sown in a soil:perlite (1:2) mixture and cold (4°C) stratified in the dark for 4 d. Germination occurred at 20°C, 160 $\mu\text{mol m}^{-2} \text{s}^{-1}$ photosynthetically active radiation (9-h photoperiod), and 70% relative humidity. At the two-leaf stage, seedlings were transplanted, one seedling per pot (70 mL), with the soil:perlite (1:2) mixture enriched with 0.14 mg of 17% MgOCaO (Vitasol) and 0.14 mg of slow-release fertilizer (Osmocote plus mini; Scotts Europe) per pot. Each pot received 25 mL of nutrient solution of the composition described (Vashisht et al., 2011). The soil was covered with black mesh with a small hole for the seedling to grow through. The mesh prevented the floating of soil material during submergence experiments. Plants were grown in climate-controlled chambers (20°C, 160 $\mu\text{mol m}^{-2} \text{s}^{-1}$ photosynthetically active radiation [9-h photoperiod], and 70% relative humidity). Plants were automatically watered each day at the start of the photoperiod. Submergence experiments were performed after plants reached a developmental stage of 10 leaves.

Experimental Conditions

Plants were completely submerged in plastic tubs (60 × 40 × 27 cm) filled to the brim with tap water and allowed to acclimatize overnight. Both darkness-only and darkness and submergence treatments took place in the same conditions as plant growth, but with the lights off (in complete darkness). Experiments were started 2 h after the start of the photoperiod. Tissue harvest was done with a low-intensity green safelight. Samples for AL, AD, and SD were harvested after 4 h of treatment. Roots and shoots were harvested separately, and the hypocotyl region (the region between the shoot base and the beginning of the first lateral root) was left out. The experiment was performed individually three times. Each time, five biological replicates, each including a pool of five individual plants, were sampled, and the tissues were flash frozen in liquid nitrogen. All samplings were completed within 30 min, minimizing the effects of circadian rhythms, and plants for each treatment were harvested simultaneously at the two chambers (light and dark chambers).

Petiole Elongation Measurements

Plants of Cvi-0 and C24 were grown as described above and, when they reached the 10-leaf developmental stage, were subjected to the same experimental conditions. From a homogenous set of plants, the leaf blades of the seventh developed leaf were marked with a pink dye. Petiole lengths were measured using a digital caliper before and after 72 h of treatment on the same petiole.

RNA Extraction and Sequencing

Plant tissue was ground with a mortar and pestle, after which the RNA was extracted using the RNeasy Plant RNA Isolation Kit (Qiagen). DNA was removed via on-column DNase digestion using the RNase-Free DNase kit (Qiagen). For RNA sequencing, for each treatment, RNA samples consisted of RNA pooled from biological replicates that showed consistent results in terms of marker gene

expression and petiole elongation response to submergence. Library preparation and sequencing (on a HiSeq 2000 device) were done commercially (Macrogen; www.macrogen.com). All treatments for each accession per organ type were bar coded in the same sequencing reaction to allow multiplexing of three samples per lane. Single-end reads of 50 bp length were obtained.

Quality Control and Read Mapping

All the sequenced libraries had Phred quality scores ranging between 30 and 40, indicating 99.9% base call accuracy. Therefore, all reads were mapped to The Arabidopsis Information Resource (TAIR) 10 Arabidopsis Col-0 genome using tophat2 with bowtie2 (Kim et al., 2013) and allowing two mismatches. Only single hits were used for further analysis. The number of reads mapping to the exons, introns, and splice VIGRs (see AS, "Materials and Methods") were determined with the R packages GenomicRanges (Lawrence et al., 2013) and Rsamtools (Morgan et al., 2013). For the exons, only reads that had no overlap with nonexonic regions (i.e. introns or intergenic; IntersectionStrict) were counted, whereas for intron and VIGR counts, overlap with neighboring genomic regions was permitted (IntersectionNotEmpty).

Differential Expression Analysis

Differential expression analysis was done with generalized linear modeling approaches of the R package edgeR (Robinson and Oshlack, 2010). Where no degrees of freedom were available, a common dispersion of 0.08 was used, which is realistic for controlled experiments with genetically identical organisms and is conservative compared with common dispersion estimates that were assessed by known housekeeping genes in the data set (0.02–0.06). Additionally, only genes with more than 1 RPKM in at least one sample were included. Differential expression upon treatment for each accession and organ was done with a model including all three conditions. Genes that responded differently in the shoot compared with the root were assessed in a full factorial model for each accession and treatment. The overall response across accessions (mean response) to the treatments was assessed in a paired design correcting for baseline differences among genotypes (i.e. an additive model with no interaction), which was done for each treatment and organ separately using tag-wise dispersions. An analogous approach was taken for the organ-dependent mean response, but with the added factor of the organ-treatment interaction.

Genotype-dependent treatment responses were determined with a full factorial model and with testing for accession-treatment effects. Here also, organs and treatments were analyzed separately and with the manual common dispersion parameter. Genes showing differentiation between tolerant and intolerant accessions were identified by contrasting the sensitive genotypes (Cvi-0, Bay-0, and Ita-0) against the tolerant genotypes (Lp2-6, Ws-2, and C24). Here, the overall response of tolerant genotypes was tested for significant difference from the overall response of the sensitive genotypes. Where the overall response of each group was determined by a paired design without an interaction term, tag-wise dispersion was used subsequently.

GO overrepresentation was assessed with the GOseq Rpackage (Young et al., 2010), which incorporates gene length biases. MDS was done with the edgeR package (Robinson and Oshlack, 2010).

WGCNA

WGCNA was used to calculate coexpressed gene modules (Langfelder and Horvath, 2008). Since gene expression shows distinct patterns in roots and shoots, they were analyzed separately in the clustering analysis. The raw count data were filtered with the RPKM method, yielding 17,525 and 15,550 genes for roots and shoots, respectively. Library size normalization was done with the edgeR package (Robinson and Oshlack, 2010), and the data were transformed in the limma package with voom function (Ritchie et al., 2015) in order to enable usage of the WGCNA package designed for microarrays. The clustering was performed with default settings, and soft thresholds of 4 and 9 were used for roots and shoots, respectively. As a representative of each module, an Eigen gene was calculated as the first principal component axis of the gene expression pattern in that module. For each gene within a module, a module membership score was computed based on the similarity of the gene to this Eigen gene.

AS

Estimation of AS and IR due to treatment or genotype effects was based on the existing TAIR 10 Col-0 annotation, using a method analogous to that of

Chang et al. (2014). Genomic regions that provide information regarding variant use (i.e. genomic regions that are transcribed in one variant but not in the alternative variant) were identified with the R package *GenomicRanges* (Lawrence et al., 2013). Reads mapping to these VIGRs were counted, allowing for overlap with neighboring genomic regions (*IntersectionNotEmpty*). Similarly, reads mapping to unambiguous intron regions were counted to assess IR.

Expected reads for each intron and VIGR were determined assuming that splice variant use and intron use does not change upon treatment or between genotypes. For instance, the expected reads for a treatment in a particular genotype would be $(VIGR_{AL} + VIGR_{AD} + VIGR_{SD}) / (Exon_{AL} + Exon_{AD} + Exon_{SD}) \times Exon_{SD}$. In case of multiple VIGRs in a single gene, they were calculated independently, whereas introns were grouped as one unit. Only introns and VIGRs with an average read count of more than 12 were included. The magnitude of AS and IR was determined by the ratio of the observed and expected reads and subsequently \log_2 transformed so that AS and IR equals 0 when observed and expected reads have equal values. Significance was estimated with a χ^2 test [$\sum((O - E)^2/E)$] and Benjamini-Hochberg corrected for multiple testing (Benjamini and Hochberg, 1995). Treatment-dependent AS and IR were assessed separately for genotypes and organs. Genotype-dependent AS and IR were assessed separately for each condition and organ. The maximum difference in splice variant usage is the highest $\log_2(obs/exp)$ minus the lowest $\log_2(obs/exp)$.

qRT-PCR

From RNA extracted with the RNeasy Plant RNA Isolation Kit (Qiagen) and treated with DNase (Qiagen), complementary DNA was made by reverse transcription (SuperScript III Reverse Transcriptase; Invitrogen) with random hexamers and including RNase inhibitor (ThermoScientific). qRT-PCR was performed in a Viia7 Real/Time PCR system (ThermoScientific) using iTaq Universal SYBR Green Supermix (Bio-Rad) in 5- μ L reaction mixtures with gene-specific primers and five reference genes (Supplemental Table S4).

Accession Number

The raw sequencing files from RNA sequencing are available in the ArrayExpress database (www.ebi.ac.uk/arrayexpress) under accession number E-MTAB-4730.

Supplemental Data

The following supplemental materials are available.

Supplemental Figure S1. Compound and darkness responses of the eight accessions in root and shoot tissues.

Supplemental Figure S2. Number of genes with an accession-dependent treatment response.

Supplemental Figure S3. GO overrepresentation of genes that vary in their response across accessions.

Supplemental Figure S4. WGCNA of shoots and roots.

Supplemental Figure S5. Genes with an organ-dependent response to the treatments.

Supplemental Figure S6. Overview of IR and AS across genotypes and upon treatments.

Supplemental Figure S7. The conserved responses in IR upon treatment in the root.

Supplemental Figure S8. The conserved responses in IR upon treatment in the shoot.

Supplemental Figure S9. Change in total transcript abundance of genes with evidence of AS upon compound, darkness, and submergence.

Supplemental Figure S10. Genes encoding important enzymatic steps of gluconeogenesis and the glyoxylate pathway.

Supplemental Figure S11. Change in petiole growth rate upon different combinations of darkness and submergence.

Supplemental Figure S12. Schematic simplification of pathways transcriptionally regulated by compound, darkness, and submergence.

Supplemental Table S1. Variation in tolerance to complete submergence in the dark of the eight accessions used in this study.

Supplemental Table S2. Summary statistics of Illumina sequencing of the mRNAseq libraries and subsequent mapping to TAIR 10 Arabidopsis genome.

Supplemental Table S3. Correlation statistics of the response of an individual genotype compared with the mean responses of all eight genotypes

Supplemental Table S4. Primers used for qRT-PCR analyses of transcript abundance.

Supplemental Data Set S1. Differential expression data from the mRNA-seq data set for all the different comparisons investigated in this study.

ACKNOWLEDGMENTS

We thank Johanna Kociemba, Ankie Ammerlaan, Rob Welschen, and Judith Koerselman for practical assistance and Reed Sorenson and Marcel van Verk for advice on mRNAseq data analyses.

Received March 24, 2016; accepted May 13, 2016; published May 15, 2016.

LITERATURE CITED

- Amthor J** (2000) The McCree-de Wit-Penning de Vries-Thornley respiration paradigms: 30 years later. *Ann Bot (Lond)* **86**: 1–20
- Angelovici R, Fait A, Fernie AR, Galili G** (2011) A seed high-lysine trait is negatively associated with the TCA cycle and slows down Arabidopsis seed germination. *New Phytol* **189**: 148–159
- Antonio C, Papke C, Rocha M, Diab H, Limami AM, Obata T, Fernie AR, van Dongen JT** (2016) Regulation of primary metabolism in response to low oxygen availability as revealed by carbon and nitrogen isotope redistribution. *Plant Physiol* **170**: 43–56
- Armstrong J, Armstrong W** (2001) An overview of the effects of phyto-toxins on *Phragmites australis* in relation to die-back. *Aquat Bot* **69**: 251–268
- Baena-González E, Rolland F, Thevelein JM, Sheen J** (2007) A central integrator of transcription networks in plant stress and energy signaling. *Nature* **448**: 938–942
- Banti V, Mafessoni F, Loreti E, Alpi A, Perata P** (2010) The heat-inducible transcription factor HsfA2 enhances anoxia tolerance in Arabidopsis. *Plant Physiol* **152**: 1471–1483
- Barding GA Jr, Béni S, Fukao T, Bailey-Serres J, Larive CK** (2013) Comparison of GC-MS and NMR for metabolite profiling of rice subjected to submergence stress. *J Proteome Res* **12**: 898–909
- Benjamini Y, Hochberg Y** (1995) Controlling the false discovery rate: a practical and powerful approach to multiple testing. *J R Stat Soc Series B Stat Methodol* **57**: 289–300
- Bernal M, Casero D, Singh V, Wilson GT, Grande A, Yang H, Dodani SC, Pellegrini M, Huijser P, Connolly EL, et al** (2012) Transcriptome sequencing identifies SPL7-regulated copper acquisition genes FRO4/FRO5 and the copper dependence of iron homeostasis in *Arabidopsis*. *Plant Cell* **24**: 738–761
- Bond DM, Wilson IW, Dennis ES, Pogson BJ, Finnegan EJ** (2009) VERNALIZATION INSENSITIVE 3 (VIN3) is required for the response of Arabidopsis thaliana seedlings exposed to low oxygen conditions. *Plant J* **59**: 576–587
- Branco-Price C, Kaiser KA, Jang CJH, Larive CK, Bailey-Serres J** (2008) Selective mRNA translation coordinates energetic and metabolic adjustments to cellular oxygen deprivation and reoxygenation in *Arabidopsis thaliana*. *Plant J* **56**: 743–755
- Brown NJ, Palmer BG, Stanley S, Hajaji H, Janacek SH, Astley HM, Parsley K, Kajala K, Quick WP, Trenkamp S, et al** (2010) C acid decarboxylases required for C photosynthesis are active in the mid-vein of the C species Arabidopsis thaliana, and are important in sugar and amino acid metabolism. *Plant J* **61**: 122–133
- Campbell MT, Proctor CA, Dou Y, Schmitz AJ, Phansak P, Kruger, GR, Zhang C, Walia H** (2015) Genetic and molecular characterization of submergence response identifies Subtol6 as a major submergence tolerance locus in maize. *PLoS ONE* **10**: e0120385

- Chang CY, Lin WD, Tu SL (2014) Genome-wide analysis of heat-sensitive alternative splicing in *Physcomitrella patens*. *Plant Physiol* **165**: 826–840
- Chang R, Jang CJH, Branco-Price C, Nghiem P, Bailey-Serres J (2012) Transient MPK6 activation in response to oxygen deprivation and re-oxygenation is mediated by mitochondria and aids seedling survival in Arabidopsis. *Plant Mol Biol* **78**: 109–122
- Chen L, Liao B, Qi H, Xie LJ, Huang L, Tan WJ, Zhai N, Yuan LB, Zhou Y, Yu LJ, et al (2015) Autophagy contributes to regulation of the hypoxia response during submergence in *Arabidopsis thaliana*. *Autophagy* **11**: 2233–2246
- Chen X, Pierik R, Peeters AJM, Poorter H, Visser EJW, Huber H, de Kroon H, Voesenek LACJ (2010) Endogenous abscisic acid as a key switch for natural variation in flooding-induced shoot elongation. *Plant Physiol* **154**: 969–977
- Christianson JA, Wilson IW, Llewellyn DJ, Dennis ES (2009) The low-oxygen-induced NAC domain transcription factor ANAC102 affects viability of Arabidopsis seeds following low-oxygen treatment. *Plant Physiol* **149**: 1724–1738
- Delgado-Alvarado A, Walker RP, Leegood RC (2007) Phosphoenolpyruvate carboxykinase in developing pea seeds is associated with tissues involved in solute transport and is nitrogen-responsive. *Plant Cell Environ* **30**: 225–235
- Dinneny JR, Long TA, Wang JY, Jung JW, Mace D, Pointer S, Barron C, Brady SM, Schiefelbein J, Benfey PN (2008) Cell identity mediates the response of Arabidopsis roots to abiotic stress. *Science* **320**: 942–945
- Eastmond PJ, Astley HM, Parsley K, Aubry S, Williams BP, Menard GN, Craddock CP, Nunes-Nesi A, Fernie AR, Hibberd JM (2015) Arabidopsis uses two gluconeogenic gateways for organic acids to fuel seedling establishment. *Nat Commun* **6**: 6659
- Ellis MH, Dennis ES, Peacock WJ (1999) Arabidopsis roots and shoots have different mechanisms for hypoxic stress tolerance. *Plant Physiol* **119**: 57–64
- Fabre N, Reiter IM, Becuwe-Linka N, Genty B, Rumeau D (2007) Characterization and expression analysis of genes encoding alpha and beta carbonic anhydrases in Arabidopsis. *Plant Cell Environ* **30**: 617–629
- Fukao T, Xu K, Ronald PC, Bailey-Serres J (2006) A variable cluster of ethylene response factor-like genes regulates metabolic and developmental acclimation responses to submergence in rice. *Plant Cell* **18**: 2021–2034
- Gaillochet C, Daum G, Lohmann JU (2015) O cell, where art thou? The mechanisms of shoot meristem patterning. *Curr Opin Plant Biol* **23**: 91–97
- Gibbs DJ, Lee SC, Isa NM, Gramuglia S, Fukao T, Bassel GW, Correia CS, Corbineau F, Theodoulou FL, Bailey-Serres J, et al (2011) Homeostatic response to hypoxia is regulated by the N-end rule pathway in plants. *Nature* **479**: 415–418
- Gibbs DJ, Isa NM, Movahedi M, Lozano-Juste J, Mendiondo GM, Berckhan S, Marín-de la Rosa N, Conde JV, Correia CS, Pearce SP, et al (2014) Nitric oxide sensing in plants is mediated by proteolytic control of group VII ERF transcription factors. *Mol Cell* **53**: 369–379
- Giuntoli B, Lee SC, Licausi F, Kosmacz M, Oosumi T, van Dongen JT, Bailey-Serres J, Perata P (2014) A trihelix DNA binding protein counterbalances hypoxia-responsive transcriptional activation in Arabidopsis. *PLoS Biol* **12**: e1001950
- Gommers CMM, Visser EJW, St Onge KR, Voesenek LACJ, Pierik R (2013) Shade tolerance: when growing tall is not an option. *Trends Plant Sci* **18**: 65–71
- Gonzali S, Loreti E, Cardarelli F, Novi G, Parlanti S, Pucciariello C, Bassolino L, Banti V, Licausi F, Perata P (2015) Universal stress protein HRU1 mediates ROS homeostasis under anoxia. *Nat Plants* **1**: 15151
- Graf A, Schlereth A, Stitt M, Smith AM (2010) Circadian control of carbohydrate availability for growth in Arabidopsis plants at night. *Proc Natl Acad Sci USA* **107**: 9458–9463
- Hartmann L, Pedrotti L, Weiste C, Fekete A, Schierstaedt J, Göttler J, Kempa S, Krischke M, Dietrich K, Mueller MJ, et al (2015) Crosstalk between two bZIP signaling pathways orchestrates salt-induced metabolic reprogramming in Arabidopsis roots. *Plant Cell* **27**: 2244–2260
- Hattori Y, Nagai K, Furukawa S, Song XJ, Kawano R, Sakakibara H, Wu J, Matsumoto T, Yoshimura A, Kitano H, et al (2009) The ethylene response factors SNORKEL1 and SNORKEL2 allow rice to adapt to deep water. *Nature* **460**: 1026–1030
- Hibberd JM, Quick WP (2002) Characteristics of C4 photosynthesis in stems and petioles of C3 flowering plants. *Nature* **415**: 451–454
- Hildebrandt TM, Nunes Nesi A, Araújo WL, Braun HP (2015) Amino acid catabolism in plants. *Mol Plant* **8**: 1563–1579
- Hsu FC, Chou MY, Peng HP, Chou SJ, Shih MC (2011) Insights into hypoxic systemic responses based on analyses of transcriptional regulation in Arabidopsis. *PLoS ONE* **6**: e28888
- Hsu PY, Harmer SL (2014) Wheels within wheels: the plant circadian system. *Trends Plant Sci* **19**: 240–249
- Huang S, Colmer TD, Millar AH (2008) Does anoxia tolerance involve altering the energy currency towards PPI? *Trends Plant Sci* **13**: 221–227
- Huijser P, Schmid M (2011) The control of developmental phase transitions in plants. *Development* **138**: 4117–4129
- Jain A, Wilson GT, Connolly EL (2014) The diverse roles of FRO family metalloendopeptidases in iron and copper homeostasis. *Front Plant Sci* **5**: 100
- Juntawong P, Girke T, Bazin J, Bailey-Serres J (2014) Translational dynamics revealed by genome-wide profiling of ribosome footprints in Arabidopsis. *Proc Natl Acad Sci USA* **111**: E203–E212
- Kazan K (2003) Alternative splicing and proteome diversity in plants: the tip of the iceberg has just emerged. *Trends Plant Sci* **8**: 468–471
- Kieber JJ, Schaller GE (2014) Cytokinins. *The Arabidopsis Book* **12**: e0168, doi/10.1199/tab.0168
- Kim D, Perteu G, Trapnell C, Pimentel H, Kelley R, Salzberg SL (2013) TopHat2: accurate alignment of transcriptomes in the presence of insertions, deletions and gene fusions. *Genome Biol* **14**: R36
- Kobayashi K, Baba S, Obayashi T, Sato M, Toyooka K, Keränen M, Aro EM, Fukaki H, Ohta H, Sugimoto K, et al (2012) Regulation of root greening by light and auxin/cytokinin signaling in Arabidopsis. *Plant Cell* **24**: 1081–1095
- Kreuzwieser J, Hauberg J, Howell KA, Carroll A, Rennenberg H, Millar AH, Whelan J (2009) Differential response of gray poplar leaves and roots underpins stress adaptation during hypoxia. *Plant Physiol* **149**: 461–473
- Langfelder P, Horvath S (2008) WGCNA: an R package for weighted correlation network analysis. *BMC Bioinformatics* **9**: 559
- Lawrence M, Huber W, Pagès H, Abouyou P, Carlson M, Gentleman R, Morgan MT, Carey VJ (2013) Software for computing and annotating genomic ranges. *PLoS Comput Biol* **9**: e1003118
- Lee KW, Chen PW, Lu CA, Chen S, Ho THD, Yu SM (2009) Coordinated responses to oxygen and sugar deficiency allow rice seedlings to tolerate flooding. *Sci Signal* **2**: ra61
- Lee SC, Mustroph A, Sasidharan R, Vashisht D, Pedersen O, Oosumi T, Voesenek LACJ, Bailey-Serres J (2011) Molecular characterization of the submergence response of the Arabidopsis thaliana ecotype Columbia. *New Phytol* **190**: 457–471
- Li J, Li G, Wang H, Wang Deng X (2011) Phytochrome signaling mechanisms. *The Arabidopsis Book* **9**: e0148, doi/10.1199/tab.0148
- Licausi F, Kosmacz M, Weits DA, Giuntoli B, Giorgi FM, Voesenek LACJ, Perata P, van Dongen JT (2011) Oxygen sensing in plants is mediated by an N-end rule pathway for protein destabilization. *Nature* **479**: 419–422
- Ljung K, Nemhauser JL, Perata P (2015) New mechanistic links between sugar and hormone signalling networks. *Curr Opin Plant Biol* **25**: 130–137
- Lokdarshi A, Conner WC, McClintock C, Li T, Roberts DM (2016) Arabidopsis CML38, a calcium sensor that localizes to ribonucleoprotein complexes under hypoxia stress. *Plant Physiol* **170**: 1046–1059
- Magneschi L, Kudahettige RL, Alpi A, Perata P (2009) Comparative analysis of anoxic coleoptile elongation in rice varieties: relationship between coleoptile length and carbohydrate levels, fermentative metabolism and anaerobic gene expression. *Plant Biol (Stuttg)* **11**: 561–573
- Malone S, Chen ZH, Bahrami AR, Walker RP, Gray JE, Leegood RC (2007) Phosphoenolpyruvate carboxykinase in Arabidopsis: changes in gene expression, protein and activity during vegetative and reproductive development. *Plant Cell Physiol* **48**: 441–450
- Mommer L, Visser EJW (2005) Underwater photosynthesis in flooded terrestrial plants: a matter of leaf plasticity. *Ann Bot (Lond)* **96**: 581–589
- Morgan M, Pages H, Obenchain V, Haydon N (2013) Rsamtools: binary alignment (BAM), FASTA, variant call (BCF) and tabix file import. R package version 1.22.0, <http://bioconductor.org/packages/release/bioc/html/Rsamtools.html>
- Mugnai S, Azzarello E, Baluska F, Mancuso S (2012) Local root apex hypoxia induces NO-mediated hypoxic acclimation of the entire root. *Plant Cell Physiol* **53**: 912–920
- Müller J, Toev T, Heisters M, Teller J, Moore KL, Hause G, Dinesh DC, Bürstenbinder K, Abel S (2015) Iron-dependent callose deposition

- adjusts root meristem maintenance to phosphate availability. *Dev Cell* **33**: 216–230
- Mustroph A, Barding GA Jr, Kaiser KA, Larive CK, Bailey-Serres J** (2014a) Characterization of distinct root and shoot responses to low-oxygen stress in *Arabidopsis* with a focus on primary C- and N-metabolism. *Plant Cell Environ* **37**: 2366–2380
- Mustroph A, Hess N, Sasidharan R** (2014b) Hypoxic energy metabolism and PPI as an alternative energy currency. In *Low-Oxygen Stress in Plants*. *Plant Cell Monographs*, Vol 21. Springer, Vienna, pp 165–184
- Mustroph A, Lee SC, Oosumi T, Zanetti ME, Yang H, Ma K, Yaghoubi-Masihi A, Fukao T, Bailey-Serres J** (2010) Cross-kingdom comparison of transcriptomic adjustments to low-oxygen stress highlights conserved and plant-specific responses. *Plant Physiol* **152**: 1484–1500
- Mustroph A, Zanetti ME, Jang CJH, Holtan HE, Repetti PP, Galbraith DW, Girke T, Bailey-Serres J** (2009) Profiling transcriptomes of discrete cell populations resolves altered cellular priorities during hypoxia in *Arabidopsis*. *Proc Natl Acad Sci USA* **106**: 18843–18848
- Narsai R, Edwards JM, Roberts TH, Whelan J, Joss GH, Atwell BJ** (2015) Mechanisms of growth and patterns of gene expression in oxygen-deprived rice coleoptiles. *Plant J* **82**: 25–40
- Narsai R, Howell KA, Carroll A, Ivanova A, Millar AH, Whelan J** (2009) Defining core metabolic and transcriptomic responses to oxygen availability in rice embryos and young seedlings. *Plant Physiol* **151**: 306–322
- Pal SK, Liput M, Piques M, Ishihara H, Obata T, Martins MCM, Sulpice R, van Dongen JT, Fernie AR, Yadav UP, et al** (2013) Diurnal changes of polysome loading track sucrose content in the rosette of wild-type *Arabidopsis* and the starchless *pgm* mutant. *Plant Physiol* **162**: 1246–1265
- Parsley K, Hibberd JM** (2006) The *Arabidopsis* *PPDK* gene is transcribed from two promoters to produce differentially expressed transcripts responsible for cytosolic and plastidic proteins. *Plant Mol Biol* **62**: 339–349
- Penfield S, Rylott EL, Gilday AD, Graham S, Larson TR, Graham IA** (2004) Reserve mobilization in the *Arabidopsis* endosperm fuels hypocotyl elongation in the dark, is independent of abscisic acid, and requires PHOSPHOENOLPYRUVATE CARBOXYKINASE1. *Plant Cell* **16**: 2705–2718
- Pracharoenwattana I, Cornah JE, Smith SM** (2007) *Arabidopsis* peroxisomal malate dehydrogenase functions in beta-oxidation but not in the glyoxylate cycle. *Plant J* **50**: 381–390
- Ritchie ME, Phipson B, Wu D, Hu Y, Law CW, Shi W, Smyth GK** (2015) limma powers differential expression analyses for RNA-seq and microarray studies. *Nucleic Acids Res* **43**: e47
- Robinson MD, Oshlack A** (2010) A scaling normalization method for differential expression analysis of RNA-seq data. *Genome Biol* **11**: R25
- Rocha M, Licausi F, Araújo WL, Nunes-Nesi A, Sodek L, Fernie AR, van Dongen JT** (2010) Glycolysis and the tricarboxylic acid cycle are linked by alanine aminotransferase during hypoxia induced by waterlogging of *Lotus japonicus*. *Plant Physiol* **152**: 1501–1513
- Santaniello A, Loreti E, Gonzali S, Novi G, Perata P** (2014) A reassessment of the role of sucrose synthase in the hypoxic sucrose-ethanol transition in *Arabidopsis*. *Plant Cell Environ* **37**: 2294–2302
- Sasidharan R, Mustroph A, Boonman A, Akman M, Ammerlaan AMH, Breit T, Schranz ME, Voeselek LACJ, van Tienderen PH** (2013) Root transcript profiling of two *Rorippa* species reveals gene clusters associated with extreme submergence tolerance. *Plant Physiol* **163**: 1277–1292
- Schröder F, Lisso J, Müssig C** (2011) EXORDIUM-LIKE1 promotes growth during low carbon availability in *Arabidopsis*. *Plant Physiol* **156**: 1620–1630
- Sheen J** (1990) Metabolic repression of transcription in higher plants. *Plant Cell* **2**: 1027–1038
- Shin DH, Cho MH, Kim TL, Yoo J, Kim JI, Han YJ, Song PS, Jeon JS, Bhoo SH, Hahn TR** (2010) A small GTPase activator protein interacts with cytoplasmic phytochromes in regulating root development. *J Biol Chem* **285**: 32151–32159
- Smeekens S, Ma J, Hanson J, Rolland F** (2010) Sugar signals and molecular networks controlling plant growth. *Curr Opin Plant Biol* **13**: 274–279
- Sorenson R, Bailey-Serres J** (2014) Selective mRNA sequestration by OLIGOURIDYLATE-BINDING PROTEIN 1 contributes to translational control during hypoxia in *Arabidopsis*. *Proc Natl Acad Sci USA* **111**: 2373–2378
- Svistonoff S, Creff A, Reymond M, Sigoillot-Claude C, Ricaud L, Blanchet A, Nussaume L, Desnos T** (2007) Root tip contact with low-phosphate media reprograms plant root architecture. *Nat Genet* **39**: 792–796
- Tang G, Zhu X, Gakiere B, Levanony H, Kahana A, Galili G** (2002) The bifunctional LKR/SDH locus of plants also encodes a highly active monofunctional lysine-ketoglutarate reductase using a polyadenylation signal located within an intron. *Plant Physiol* **130**: 147–154
- Taylor L, Nunes-Nesi A, Parsley K, Leiss A, Leach G, Coates S, Wingler A, Fernie AR, Hibberd JM** (2010) Cytosolic pyruvate, orthophosphate dikinase functions in nitrogen remobilization during leaf senescence and limits individual seed growth and nitrogen content. *Plant J* **62**: 641–652
- Usadel B, Bläsing OE, Gibon Y, Retzlaff K, Höhne M, Günther M, Stitt M** (2008) Global transcript levels respond to small changes of the carbon status during progressive exhaustion of carbohydrates in *Arabidopsis* rosettes. *Plant Physiol* **146**: 1834–1861
- Usami T, Mochizuki N, Kondo M, Nishimura M, Nagatani A** (2004) Cryptochromes and phytochromes synergistically regulate *Arabidopsis* root greening under blue light. *Plant Cell Physiol* **45**: 1798–1808
- van Dongen JT, Licausi F** (2015) Oxygen sensing and signaling. *Annu Rev Plant Biol* **66**: 345–367
- Van Eck WHJM, van de Steeg HM, Blom CWPM, de Kroon H** (2004) Is tolerance to summer flooding correlated with distribution patterns in river floodplains? A comparative study of 20 terrestrial grassland species. *Oikos* **107**: 393–405
- van Veen H, Akman M, Jamar DCL, Vreugdenhil D, Kooiker M, van Tienderen P, Voeselek LACJ, Schranz ME, Sasidharan R** (2014a) Group VII ethylene response factor diversification and regulation in four species from flood-prone environments. *Plant Cell Environ* **37**: 2421–2432
- van Veen H, Mustroph A, Barding GA, Vergeer-van Eijk M, Welschen-Evertman RAM, Pedersen O, Visser EJW, Larive CK, Pierik R, Bailey-Serres J, et al** (2013) Two *Rumex* species from contrasting hydrological niches regulate flooding tolerance through distinct mechanisms. *Plant Cell* **25**: 4691–4707
- van Veen H, Vashisht D, Voeselek LACJ, Sasidharan R** (2014b) Different survival strategies amongst plants to cope with underwater conditions. In *Low-Oxygen Stress in Plants*. *Plant Cell Monographs*, Vol 21. Springer, Vienna, pp 329–349
- Vashisht D, Hesselink A, Pierik R, Ammerlaan JMH, Bailey-Serres J, Visser EJW, Pedersen O, van Zanten M, Vreugdenhil D, Jamar DCL, et al** (2011) Natural variation of submergence tolerance among *Arabidopsis thaliana* accessions. *New Phytol* **190**: 299–310
- Vervuren P, Blom C, de Kroon H** (2003) Extreme flooding events on the Rhine and the survival and distribution of riparian plant species. *J Ecol* **91**: 135–146
- Voeselek LACJ, Bailey-Serres J** (2015) Flood adaptive traits and processes: an overview. *New Phytol* **206**: 57–73
- Voeselek LACJ, Rijnders JHGM, Peeters AJM, van de Steeg HM, de Kroon H** (2004) Plant hormones regulate fast shoot elongation under water: from genes to communities. *Ecology* **85**: 16–27
- Voeselek LACJ, Sasidharan R** (2013) Ethylene—and oxygen signalling—drive plant survival during flooding. *Plant Biol (Stuttg)* **15**: 426–435
- Voeselek LACJ, van Veen H, Sasidharan R** (2014) Learning from nature: the use of non-model species to identify novel acclimations to flooding stress. *AoB Plants* **6**: plu016
- Watanabe M, Balazadeh S, Tohge T, Erban A, Giavalisco P, Kopka J, Mueller-Roeber B, Fernie AR, Hoefgen R** (2013) Comprehensive dissection of spatiotemporal metabolic shifts in primary, secondary, and lipid metabolism during developmental senescence in *Arabidopsis*. *Plant Physiol* **162**: 1290–1310
- Weits DA, Giuntoli B, Kosmacz M, Parlanti S, Hubberten HM, Riegler H, Hoefgen R, Perata P, van Dongen JT, Licausi F** (2014) Plant cysteine oxidases control the oxygen-dependent branch of the N-end-rule pathway. *Nat Commun* **5**: 3425
- Xu K, Xu X, Fukao T, Canlas P, Maghirang-Rodriguez R, Heuer S, Ismail AM, Bailey-Serres J, Ronald PC, Mackill DJ** (2006) Sub1A is an ethylene-response-factor-like gene that confers submergence tolerance to rice. *Nature* **442**: 705–708
- Young MD, Wakefield MJ, Smyth GK, Oshlack A** (2010) Gene ontology analysis for RNA-seq: accounting for selection bias. *Genome Biol* **11**: R14
- Zabalza A, van Dongen JT, Froehlich A, Oliver SN, Faix B, Gupta KJ, Schmäzlin E, Igal M, Orcaray L, Royuela M, et al** (2009) Regulation of respiration and fermentation to control the plant internal oxygen concentration. *Plant Physiol* **149**: 1087–1098
- Zhu X, Tang G, Galili G** (2002) The activity of the *Arabidopsis* bifunctional lysine-ketoglutarate reductase/saccharopine dehydrogenase enzyme of lysine catabolism is regulated by functional interaction between its two enzyme domains. *J Biol Chem* **277**: 49655–49661